MODELING AND IDENTIFICATION OF A UAV WITH A FLEXIBLE WING

AEROSPACE TECHNOLOGY CONGRESS 2019
SUSTAINABLE AEROSPACE INNOVATION IN A GLOBALISED WORLD
FT2019

Prof. Góes L. C. S., Silva R.A.G, Zuniga, D.F.C., Barbosa, R.C.M.G. and Souza A.G.

goes@ita.br

Technological Institute of Aeronautics (ITA) - Department of Mechanical Engineering (IEM)

São José dos Campos, São Paulo - Brazil.

OCTOBER 2019

L.S.A.
Laboratório de Sistemas Aeronáuticos
Aeronautical Systems Laboratory

AEROSPACE TECHNOLOGY CONGRESS 2019
SUSTAINABLE AEROSPACE INNOVATION IN A GLOBALISED WORLD
FT2019

- INTRODUCTION
- THE EOLO UAV
- IDENTIFICATION
- WIND TUNEL CAMPAIGN
- IN-FLIGHT CAMPAIGN
- CONCLUSION

L.S.A.
Laboratório de Sistemas Aeronáuticos
Aeronautical Systems Laboratory

- INTRODUCTION
- THE EOLO UAV
- IDENTIFICATION
- WIND TUNEL CAMPAIGN
- IN-FLIGHT CAMPAIGN
- CONCLUSION

AEROSPACE TECHNOLOGY CONGRESS 2019
SUSTAINABLE AEROSPACE INNOVATION IN A GLOBALISED WORLD
FT2019

INTRODUCTION

ITA – FINEP/VINNOVA PROJECT

This paper resumes preliminary results of the FINEP/VINNOVA project "*Sensing, Acquisition, and Identification of Flight Dynamic Systems of Sub-Scale Aircraft Prototypes*.“

This project aims to develop methodology for flight testing of remotely piloted aircraft (ARP), as demonstrators of subscale aeronautical concepts. In particular to develop inflight aeroelastic tests of flexible wing aircraft, and subscale aircraft operating at high angle attack.

L.S.A.
Laboratório de Sistemas Aeronáuticos
Aeronautical Systems Laboratory

INTRODUCTION

THE EOLO UAV

IDENTIFICATION

WIND TUNEL CAMPAIGN

IN-FLIGHT CAMPAIGN

CONCLUSION

THE EOLO UAV - instrumentation

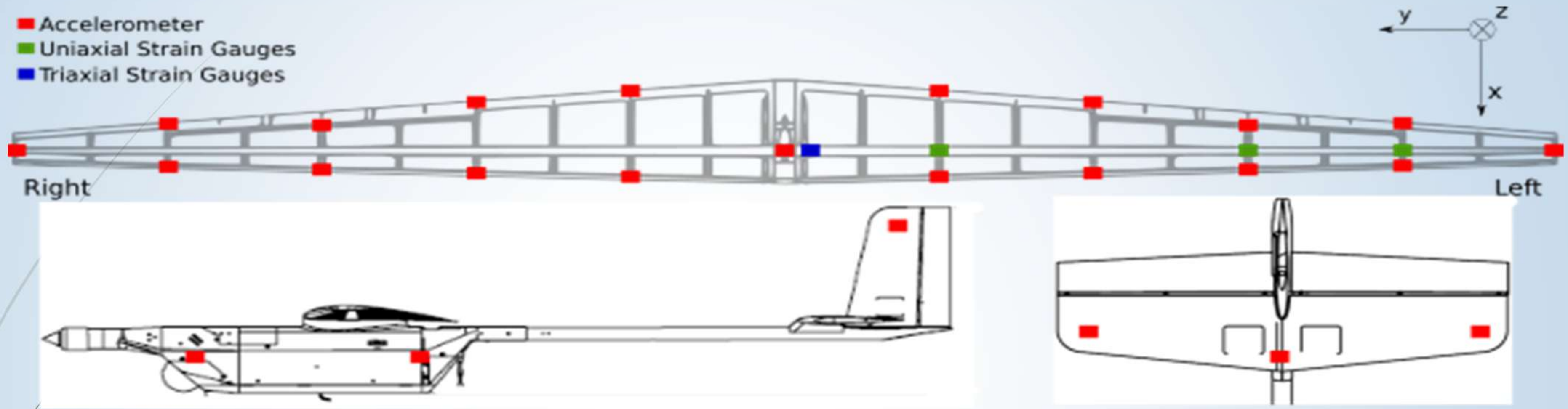

Table 1 – Geometry and mass Parameters

Parameters	Symbol	Values
Wing area	S	$0.85\ m^2$
Wing chord	$\bar{c}$	0.23 m
Wing span	b	4.00 m
Aspect ratio		19
Fuselage length		1.89 m
Wing mass	m_w	2 kg
total mass	m_t	9 kg

Table 2 – Characteristics of the main lifting surfaces of EOLO.

	Wing	Horizontal Stabilizer	Vertical Stabilizer
Span	4 m	0.70 m	0.30 m
Root chord	0.32 m	0.22 m	0.16 m
Tip Chord	0.10 m	0.22 m	0.16 m
Aspect ratio	18.91	3.68	0.72
Taper ratio	0.31	0.72	0.82
Profile	S2091-101-83	NACA 0012	NACA 0012

AEROSPACE TECHNO
SUSTAINABLE AEROSPACE INNO
FT2019

THE EOLO UAV – general overview

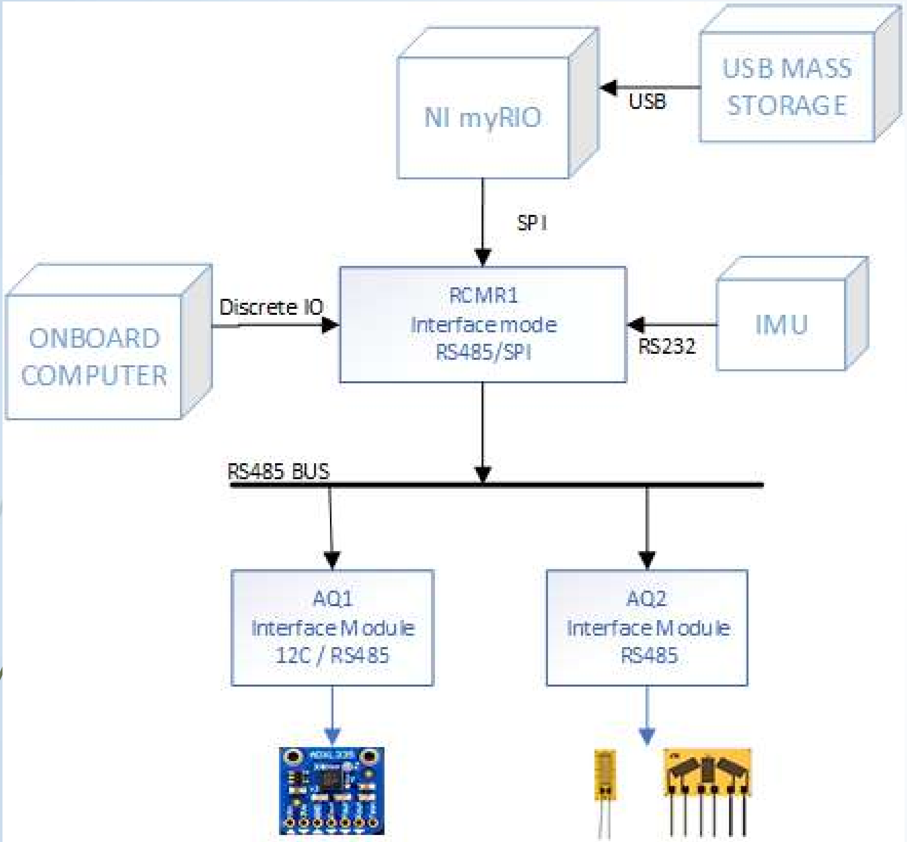

The heart of the data acquisition system architecture, is an on-board computer and control system (NI/MyRio) retrieving information of all sensors onboard the air craft, a microcomputer (FlightTech SNC-200), an anemometric system (SpaceAge Subminiature Air Data Boom 101100), an inertial unit, accelerometers, strain gauges (CEA-06-125UW-350), strain rosettes (CEA-06-250UR-350), electrical actuators and angular positions sensors.

THE EOLO UAV – mass properties measurements

Accurate values of the inertia moments and center of gravity (CG) were measured in the Mass Properties Lab at the Institute of Aeronautics and Space (IAE), using the Space Electronics device, Model KSR 1320. The principle of measurement of this device is based on the inverted torsion pendulum concepts. The measurement procedure is shown in the figure.

X Inertial moment	I_{xx}	2.53 kg m^2
Y Inertial moment	I_{yy}	1.60 kg m^2
Z Inertial moment	I_{zz}	3.96 kg m^2

THE EOLO UAV – structural dynamics mathematical model

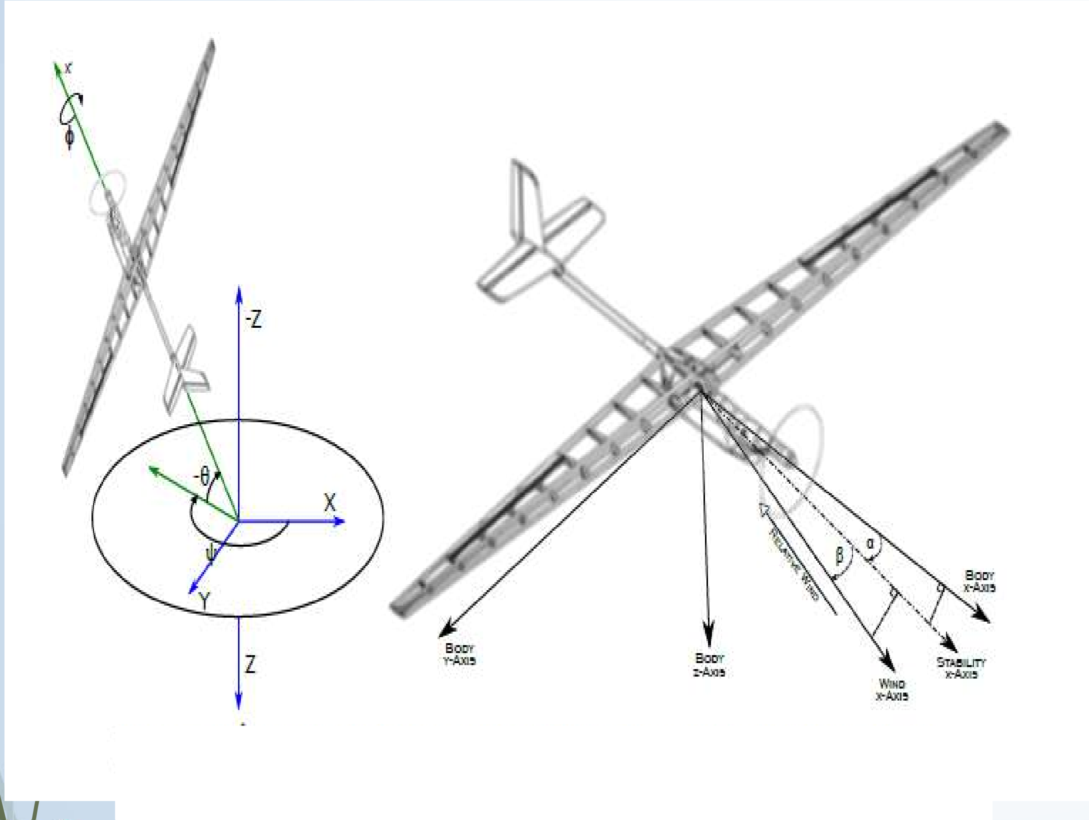

Starting from the hypothesis that the airplane is considered a continuous elastic body it is possible to obtain its equations using the **Lagrange Equations** and the **principle of the virtual work**.

The figure shows the frames defined with respect to the body. The first hypothesis that allows writing the structural displacement in a point of the structure of the aircraft like an infinite sum of the contributions of its normal modes:

$$\vec{d}(x,y,z)=\sum_{i=1}^{\infty}\vec{\varphi}_i(x,y,z)\eta_i(t)$$

THE EOLO UAV - mathematical model

$$
\begin{aligned}
&\dot{u} - rv + qw + gsen(\theta) = \frac{X}{M} \\
&\dot{v} - pw + ru + gsen(\phi)cos(\theta) = \frac{Y}{M} \\
&\dot{w} - qu + pv + gcos(\phi)cos(\theta) = \frac{Z}{M} \\
&I_{xx}\dot{p} - (I_{xy}\dot{q} + I_{xz}\dot{r}) + (I_{zz} - I_{yy})qr + (I_{xy}r - I_{xz}q)p + (r^2 - q^2)I_{yz} = L \\
&I_{yy}\dot{q} - (I_{xy}\dot{p} + I_{yz}\dot{r}) + (I_{xx} - I_{zz})pr + (I_{yz}p - I_{xy}r)q + (p^2 - r^2)I_{xz} = M \\
&I_{zz}\dot{r} - (I_{xy}\dot{p} + I_{yz}\dot{q}) + (I_{yy} - I_{xx})pq + (I_{xz}q - I_{zy}r)q + (q^2 - p^2)I_{xy} = N \\
&\ddot{\eta}_i + 2\zeta_i\omega_i\dot{\eta}_i + \omega_i^2\eta_i = \frac{Q_i}{M_i}
\end{aligned}
$$

The first six equations are described in relation to the body reference axis and are formally equivalent to the classical equations of the rigid body motion. The last expression is the structural response model in terms of the **modal deflectios,** $\boldsymbol{\eta_i}$. The model has $\boldsymbol{6 + n_F}$ **dof**, where n_F is the number of flexible modes retained in the model. Q_i represents the generalized forces acting in the i-th structural mode and has aerodynamic origin.

THE EOLO UAV – aerodynamica model

The aerodynamic forces are assumed to be composed of a superposition of forces and moments due to the rigid body motion (labeled R) and due to the flexible response (envelope F). The same strategy is adopted for the generalized aerodynamic loads Q_i acting on the flexible degrees of freedom.

$$X = X_R + X_F \quad \mathfrak{L} = \mathfrak{L}_R + \mathfrak{L}_F \quad Q_i = Q_{iR} + Q_{iF}$$
$$Y = Y_R + Y_F \quad \mathfrak{M} = \mathfrak{M}_R + \mathfrak{M}_F$$
$$Z = Z_R + Z_F \quad \mathfrak{N} = \mathfrak{N}_R + \mathfrak{N}_F$$

From the strip theory:

$$L = \frac{1}{2}\rho V^2 S_{ref} \left(C_{LR} + C_{LF}\right)$$

The coefficient of lift is:

$$C_{LR} = C_{L0} + C_{L\alpha}\alpha + C_{L\delta}\delta + \frac{c}{2V}(C_{Lq} + C_{L\dot{\alpha}})$$

THE EOLO UAV - mathematical model

The coefficients for the structural dynamics are expressed as:

$$C_{LF} = \sum_{i=1}^{n} \left(C_{L\eta_{Li}} \eta_i + \frac{c}{2V} C_{L\dot{\eta}_i} \dot{\eta}_i \right)$$

$$\begin{aligned} X &= \bar{q}S(C_{XR} + C_{XF}) & \mathfrak{L} &= \bar{q}Sb(C_{\mathfrak{L}R} + C_{\mathfrak{L}F}) \\ Y &= \bar{q}S(C_{YR} + C_{YF}) & \mathfrak{M} &= \bar{q}Sb(C_{\mathfrak{M}R} + C_{\mathfrak{M}F}) \\ Z &= \bar{Q}S(C_{ZR} + C_{ZF}) & \mathfrak{N} &= \bar{q}Sb(C_{\mathfrak{N}R} + C_{\mathfrak{N}F}) \end{aligned}$$

The aeroelastic coefficients $C_{L\eta L}$ and $C\ (\dot{\eta}i)$ are obtained by analytical expressions as developed in the reference WASZAK and SCHMIDT, 1988 or estimated by means of parameter estimation from in-flight test data (Pfifer and Danowsky, 2016).

These sums are added linearly to the equations of rigid body motion of the aircraft, so that no major modifications are required for applications of the same identification methods used for rigid body dynamics.

THE EOLO UAV - longitudinal dynamics

The longitudinal dynamics is a special case, where $p = r = v = 0$. The motion is restricted to the plane os symmetry, oxz, like shown the figure.

The longitudinal motion is normally represented by small displacements from an equilibrium (unaccelerated) flight condition in the longitudinal plane. An approximation of short period dynamics are presented below according to the work of Pfifer H., and Danowsky B.P. (2016)

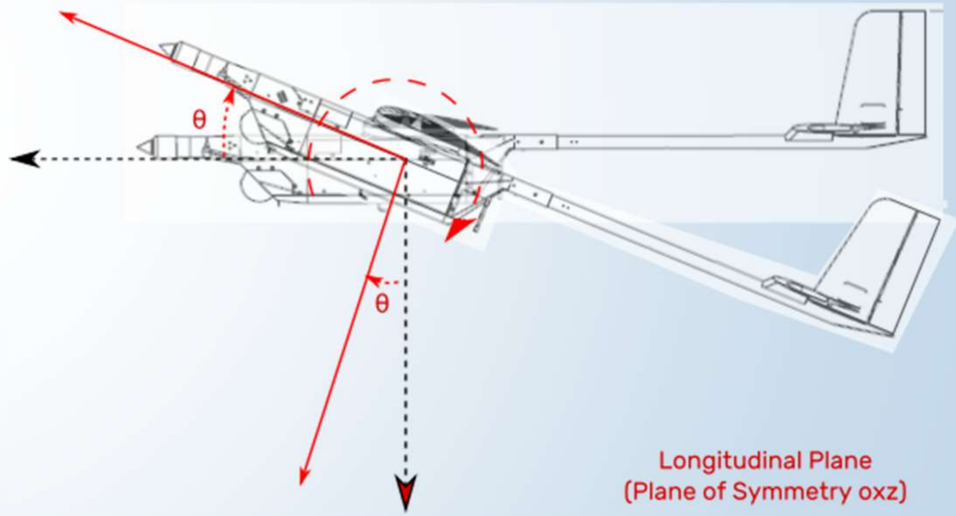

$$\begin{bmatrix} \dot{\alpha} \\ \dot{\theta} \\ \dot{q} \\ \dot{\eta}_1 \\ \ddot{\eta}_1 \end{bmatrix} = \begin{bmatrix} Z_\alpha/U_0 & 0 & 1+Z_q/U_0 & Z_{\eta_1}/U_0 & Z_{\dot{\eta}_1}/U_0 \\ 0 & 0 & 1 & 0 & 0 \\ M_\alpha & 0 & M_q & M_{\eta_1} & M_{\dot{\eta}_1} \\ 0 & 0 & 0 & 0 & 1 \\ \Xi_{1\alpha} & 0 & \Xi_{1q} & \Xi_{1\eta 1} - \omega_1^2 & \Xi_{1\dot{\eta}1} - 2\omega_1\zeta_1 \end{bmatrix} \begin{bmatrix} \alpha \\ \theta \\ q \\ \eta_1 \\ \dot{\eta}_1 \end{bmatrix} + \begin{bmatrix} Z_{\delta e}/U_0 \\ 0 \\ M_{\delta e} \\ 0 \\ \Xi_{1\delta 1} \end{bmatrix} \delta_e$$

AEROSPACE TECHNOLOGY CONGRESS 2019
SUSTAINABLE AEROSPACE INNOVATION IN A GLOBALISED WORLD
FT2019

L.S.A.
Laboratório de Sistemas Aeronáuticos
Aeronautical Systems Laboratory

UAV - EOLO

AEROSPACE TECHNOLOGY CONGRESS 2019
SUSTAINABLE AEROSPACE INNOVATION IN A GLOBALISED WORLD
FT2019

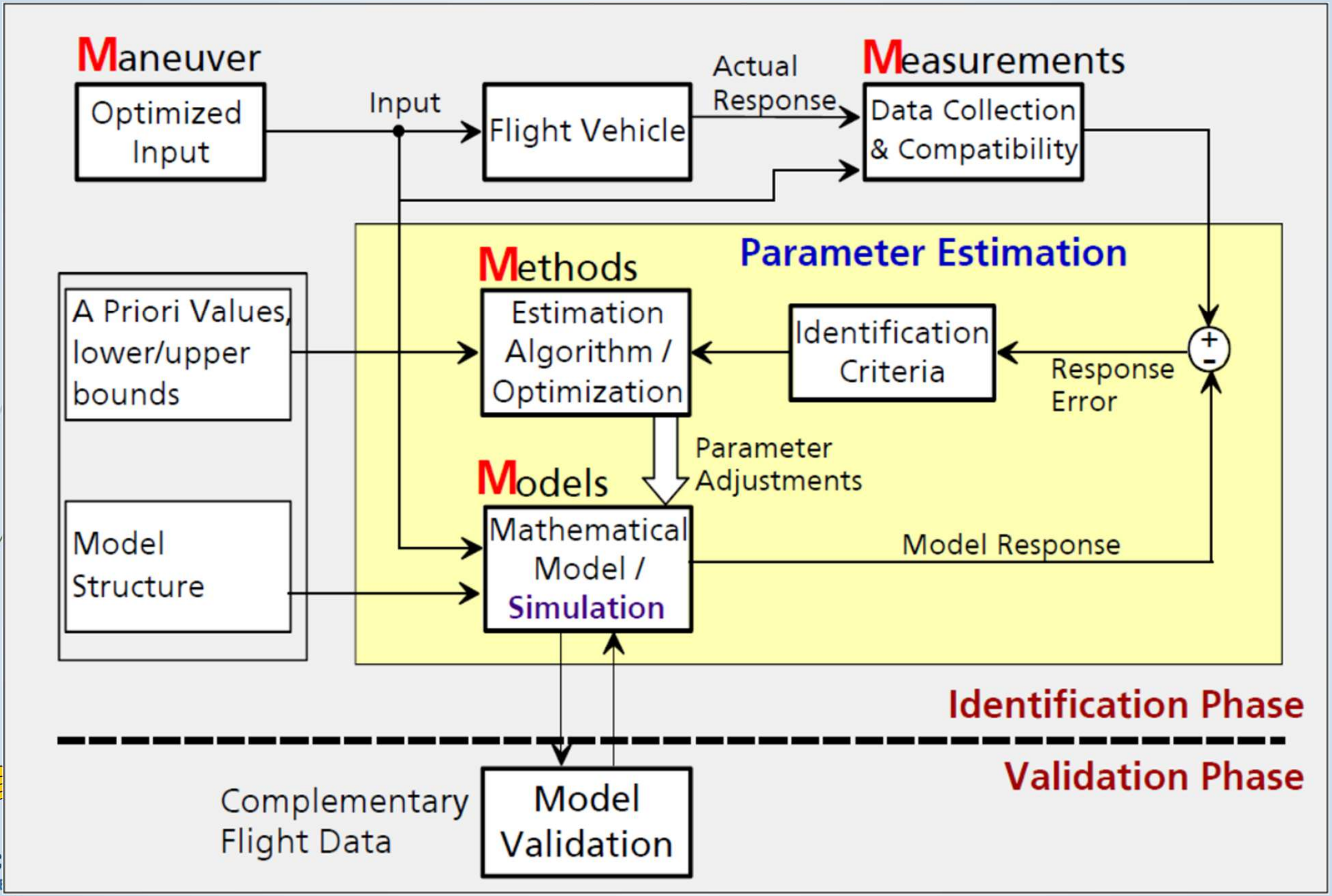

Maneuver
Optimized Input
Input
Flight Vehicle
Actual Response
Measurements
Data Collection & Compatibility
Parameter Estimation
Methods
A Priori Values, lower/upper bounds
Estimation Algorithm / Optimization
Identification Criteria
+
-
Response Error
Parameter Adjustments
Models
Model Structure
Mathematical Model / Simulation
Model Response
Identification Phase
Validation Phase
Complementary Flight Data
Model Validation

L.S.A.
Laboratório de Sistemas Aeronáuticos
Aeronautical Systems Laboratory

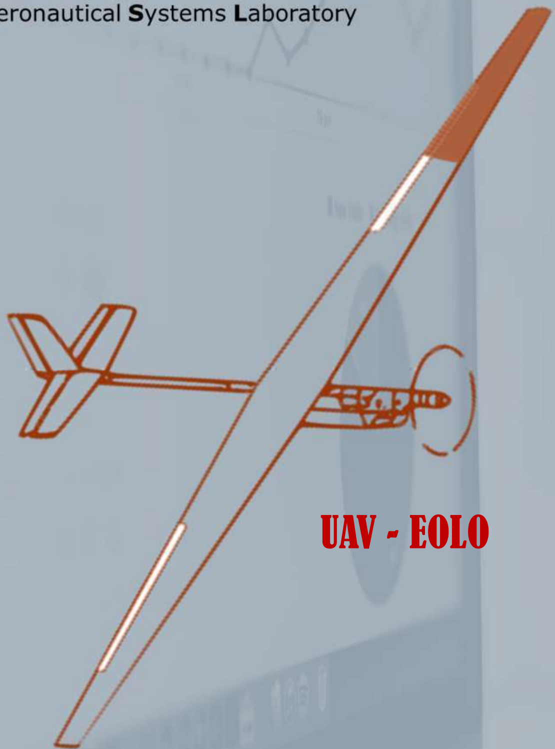

- IDENTIFICATION
- Aerodynamics
- Subspace method
- Modal - GVT EMA
- Modal - GVT OMA

AEROSPACE TECHNOLOGY CONGRESS 2019
SUSTAINABLE AEROSPACE INNOVATION IN A GLOBALISED WORLD
FT2019

IDENTIFICATION – aerodynamic (EKF method)

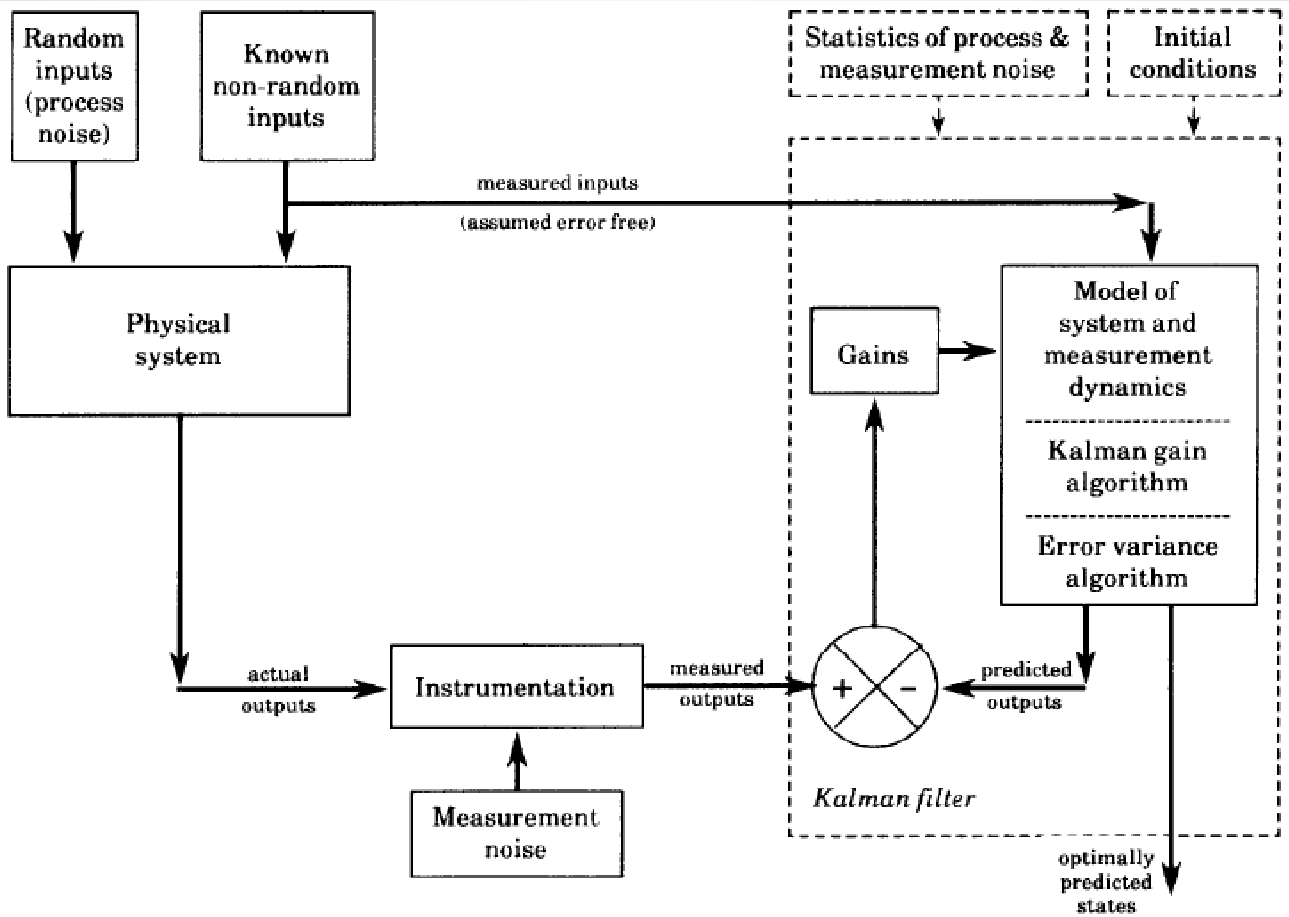

ESDU **88039**

IDENTIFICATION – aerodynamic (EKF method)

For the measurement of states it was used a simulator of the longitudinal dynamics of the Eolo. This simulator was create in a MatLab software code. For this scenario only the states α and q are considered measurable.

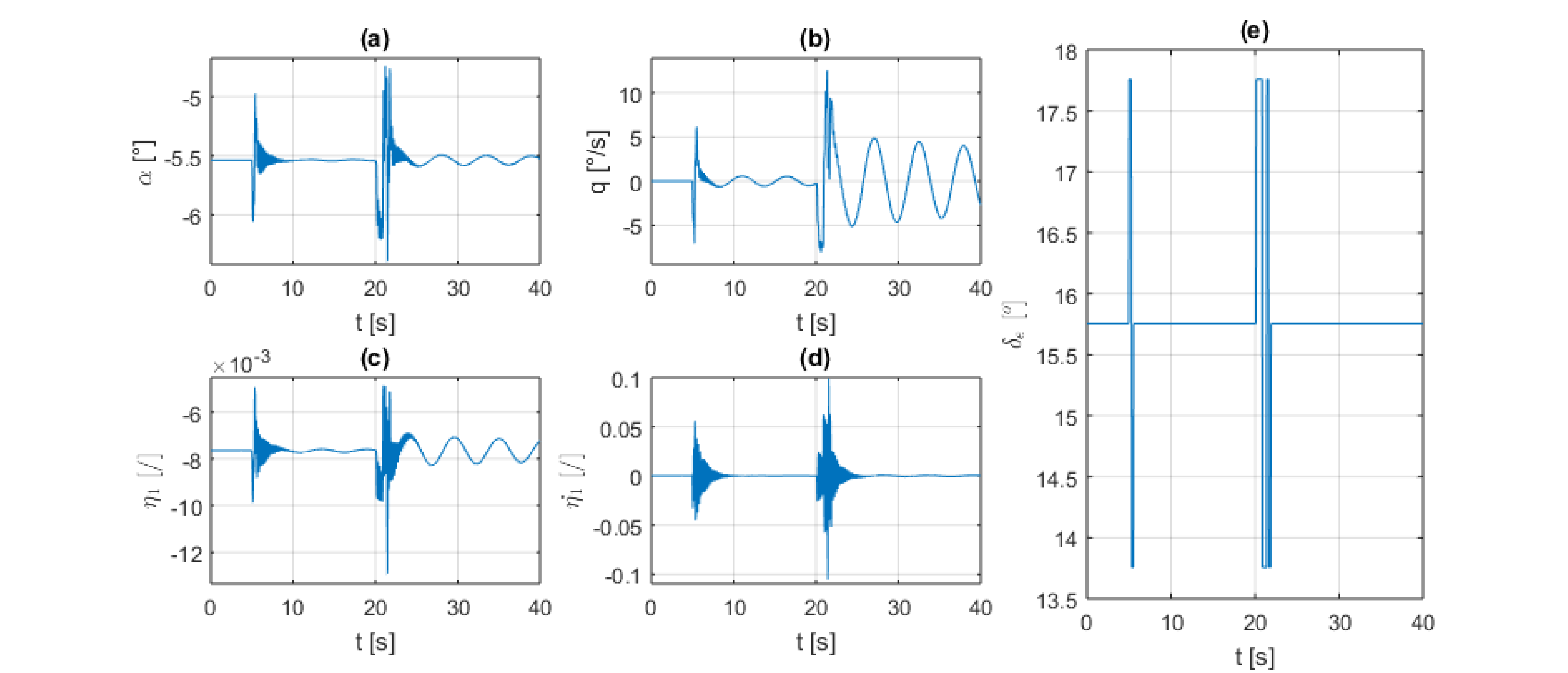

AEROSPACE TECHNOLOGY CONGRESS 2019
SUSTAINABLE AEROSPACE INNOVATION IN A GLOBALISED WORLD
FT2019

IDENTIFICATION – aerodynamic (EKF method)

Applying the Kalman filter to estimates the states:

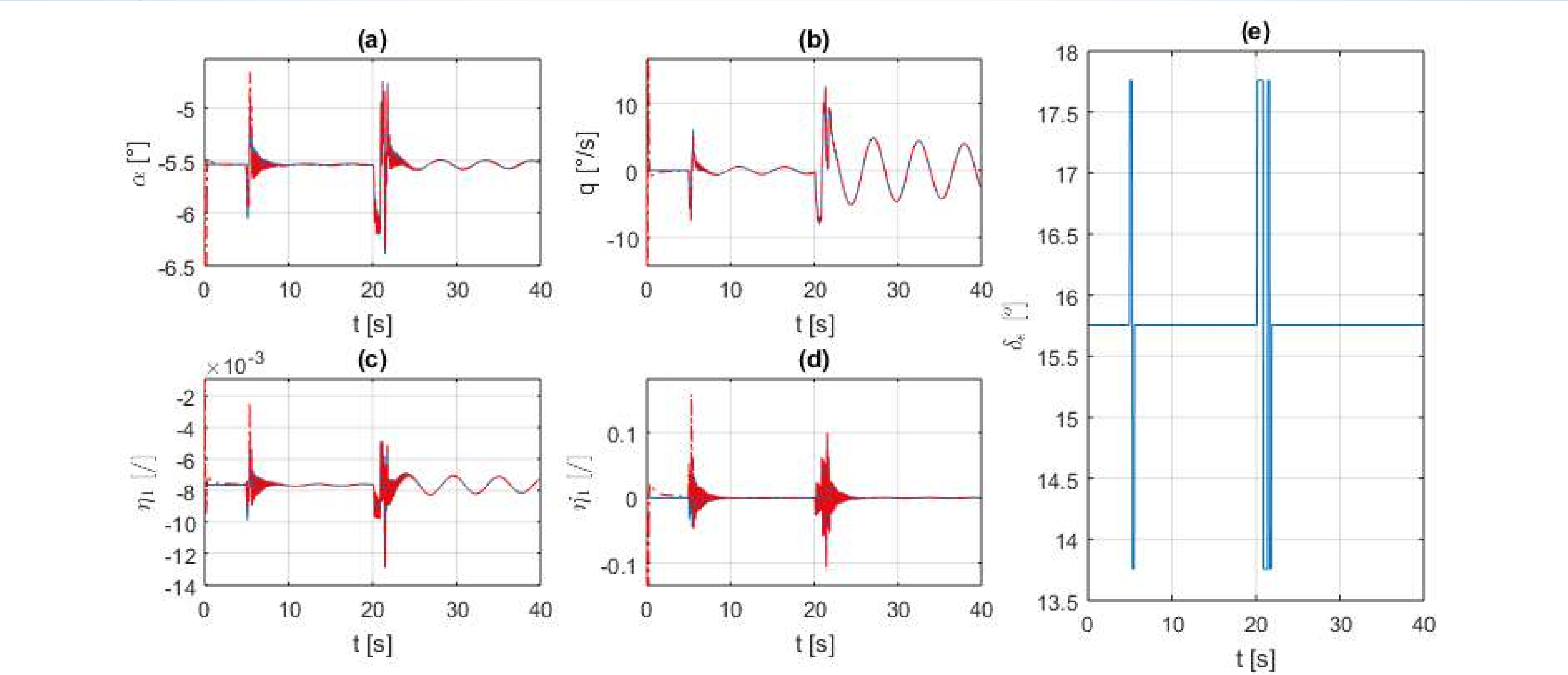

IDENTIFICATION – aerodynamic (EKF method)

Applying the Kalman filter to estimates the aerodynamics parameters:

No.	Parameter	Std. deviation	Relative Std. Dev (%)
1	6.68398e+00	1.0694e-02	0.16
2	-1.88616e+01	3.1988e-03	0.02
3	-1.15850e+00	1.4106e-04	0.01
4	-7.01587e+00	8.9064e-04	0.01
5	-4.62969e+01	2.6610e-02	0.06
6	-1.52836e+02	8.4089e-03	0.01
7	-7.30961e-01	4.3959e-04	0.06
8	-5.04775e+01	2.5538e-03	0.01

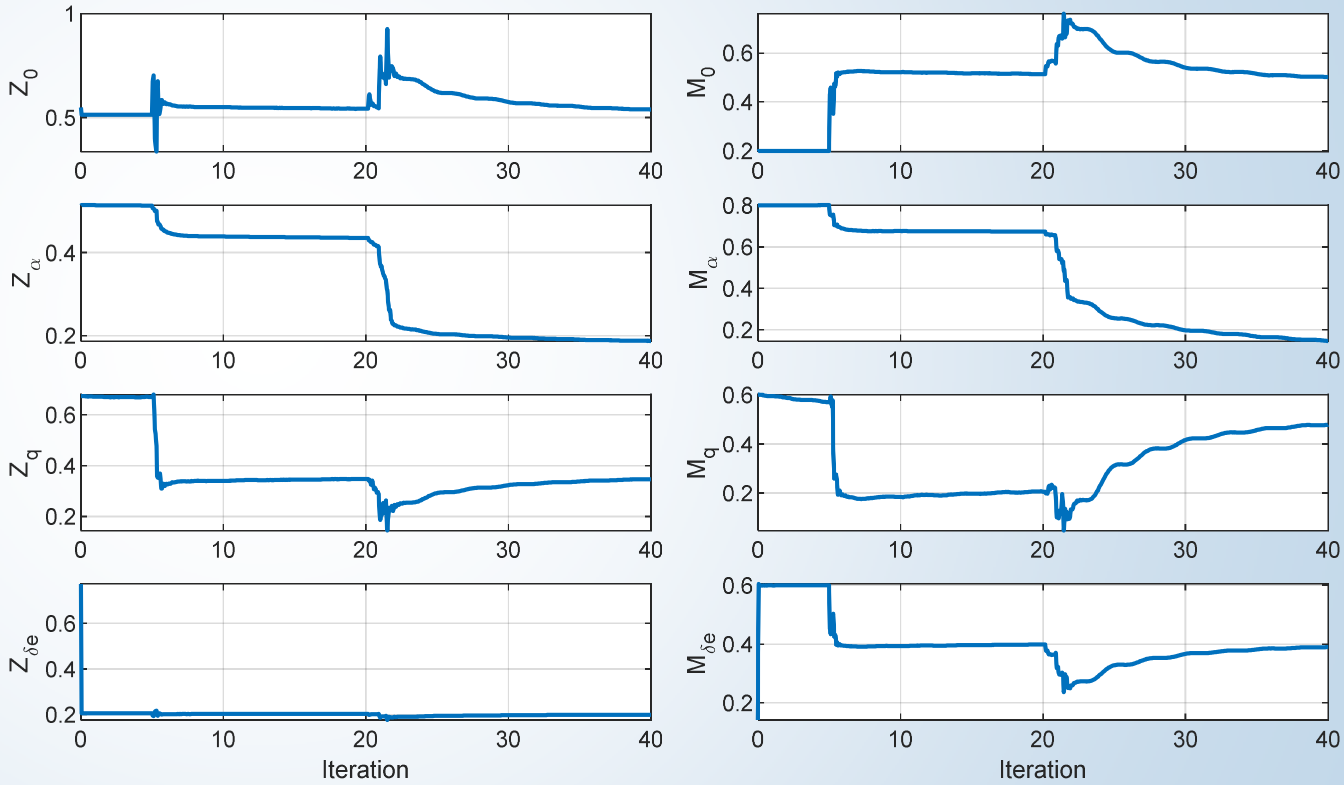

L.S.A.
Laboratório de Sistemas Aeronáuticos
Aeronautical Systems Laboratory

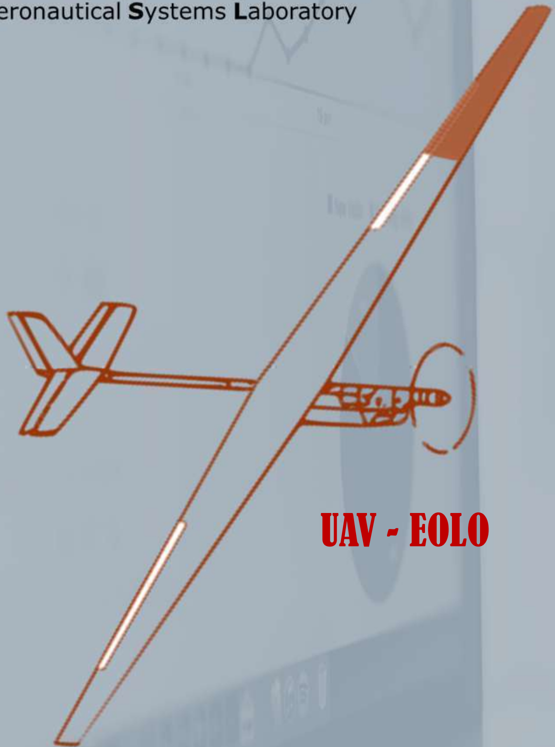

- IDENTIFICATION
- Aerodynamics
- Subspace method
- Modal - GVT EMA
- Modal - GVT OMA

AEROSPACE TECHNOLOGY CONGRESS 2019
SUSTAINABLE AEROSPACE INNOVATION IN A GLOBALISED WORLD
FT2019

MODELING – A preliminary UAS model

It was implemented in MATLAB/SIMULINK a simulation environment from previous estimates of the UAS model parameter just to provide synthetic data to perform a closed-loop system identification since that real experimental data not available yet.

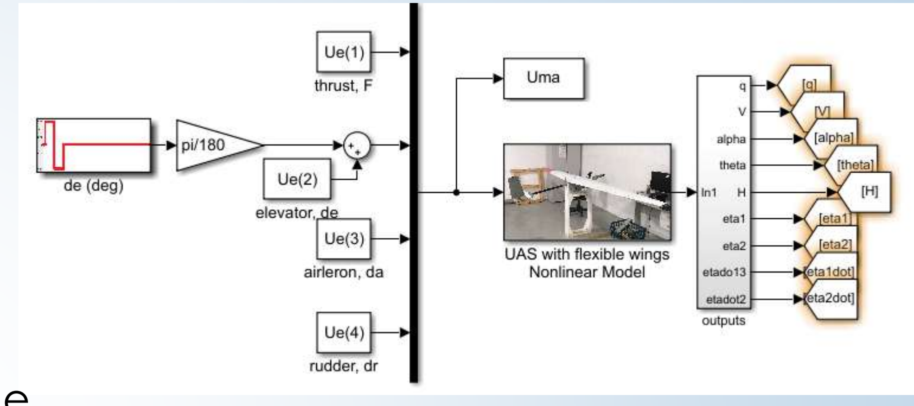

Trimmed values in equilibrium ("trim") condition of the straight and level cruise at velocity V=25m/s and altitude H=1100m.

```
Xe_ =

  9×4 cell array

    {'p (rad/s)'  }    {[      0]}    {'p (deg/s)'  }    {[      0]}
    {'q (rad/s)'  }    {[      0]}    {'q (deg/s)'  }    {[      0]}
    {'r (rad/s)'  }    {[      0]}    {'r (deg/s)'  }    {[      0]}
    {'V (m/s)'    }    {[     25]}    {'V (m/s)'    }    {[     25]}
    {'alpha (rad)'}    {[-0.0127]}    {'alpha (deg)'}    {[-0.7268]}
    {'beta (rad)' }    {[      0]}    {'beta (deg)' }    {[      0]}
    {'phi (rad)'  }    {[      0]}    {'phi (deg)'  }    {[      0]}
    {'theta (rad)'}    {[-0.0127]}    {'theta (deg)'}    {[-0.7268]}
    {'H (m)'      }    {[   1100]}    {'H (m)'      }    {[   1100]}
```

```
Ue_ =

  5×4 cell array

    {'dF(N)'  }    {[0.0537]}    {'dF(N)'  }    {[0.0537]}
    {'F(N)'   }    {[5.3711]}    {'F(N)'   }    {[5.3711]}
    {'de(rad)'}    {[0.0078]}    {'de(deg)'}    {[0.4446]}
    {'da(rad)'}    {[     0]}    {'da(deg)'}    {[     0]}
    {'dr(rad)'}    {[     0]}    {'dr(deg)'}    {[     0]}
```

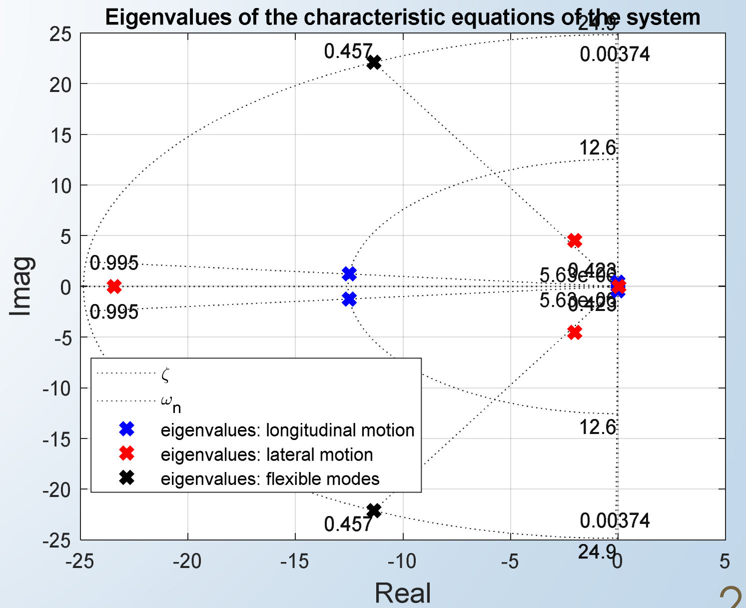

AEROSPACE TECHNOLOGY CONGRESS 2019
SUSTAINABLE AEROSPACE INNOVATION IN A GLOBALISED WORLD
FT2019

A velocity root-locus for UAS

The eigenvalues of the vehicle dynamics corresponding to a true velocity from 13m/s to 61m/s. In this case, the flutter phenomenon can not be observed yet because only one flexible mode was inserted in the simulation environment.

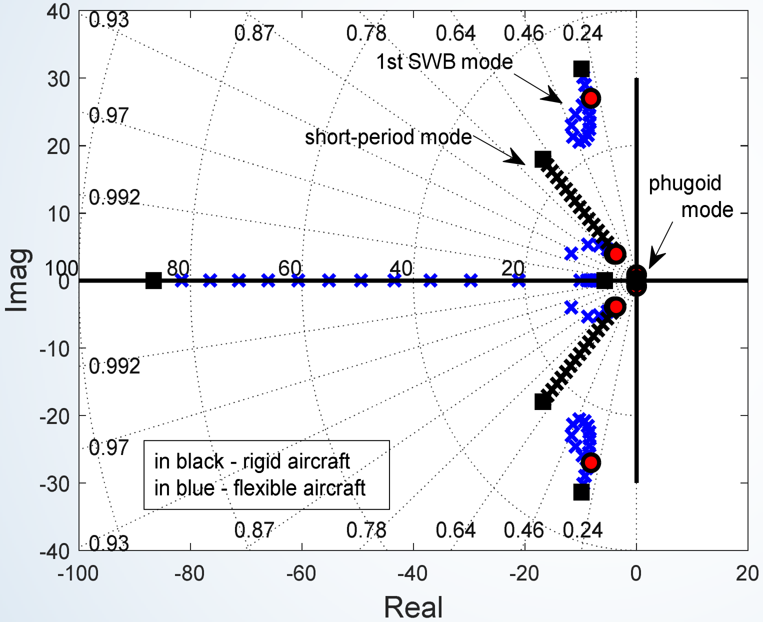

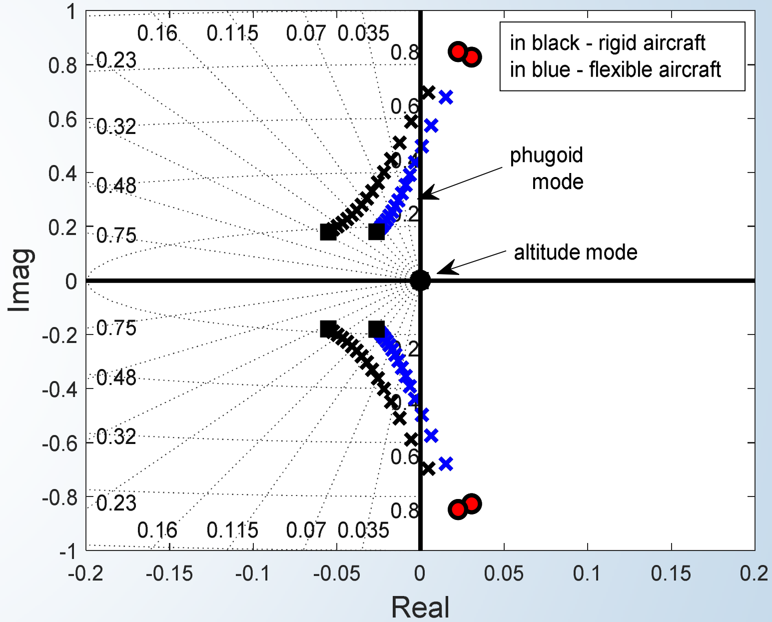

As shown, if the aircraft is flexible the rigid modes are influenced providing more damping to short-period mode. Initially, the phugoid mode is unstable in both open-loop cases, in the same way, the damping increase with true velocity variations.

Trust-to-state-variables **frequency response**

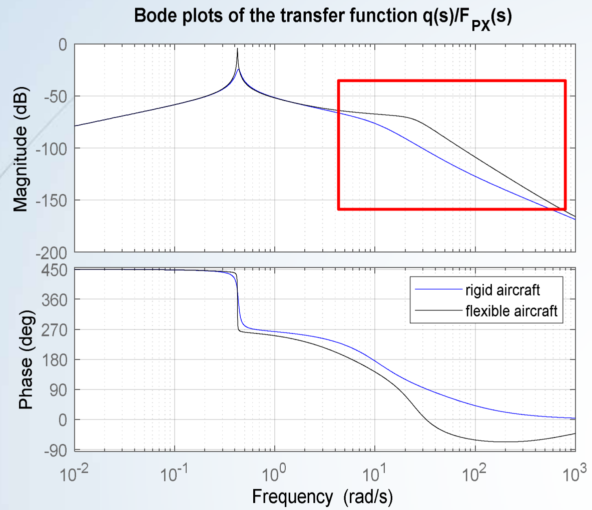

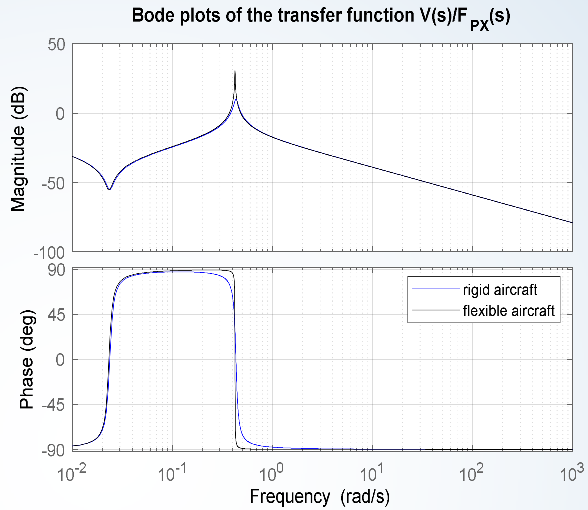

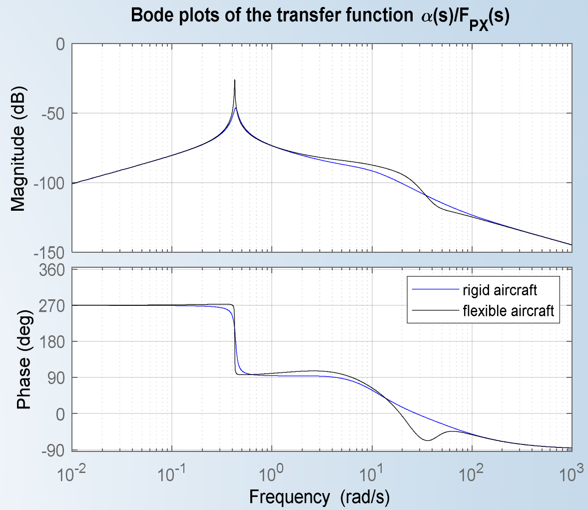

Both the magnitude and phase plots show the longitudinal motion approximation for the flight trim condition at V=25m/s and H=1100m.

Note that the flexible mode affect most significantly the pitch-rate and the pitch-attitude responses.

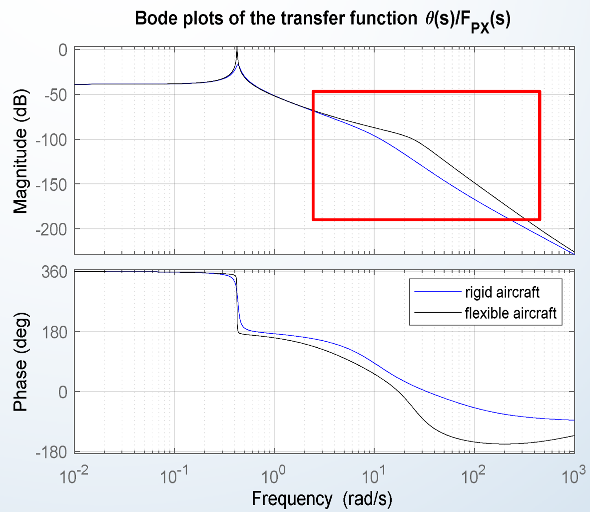

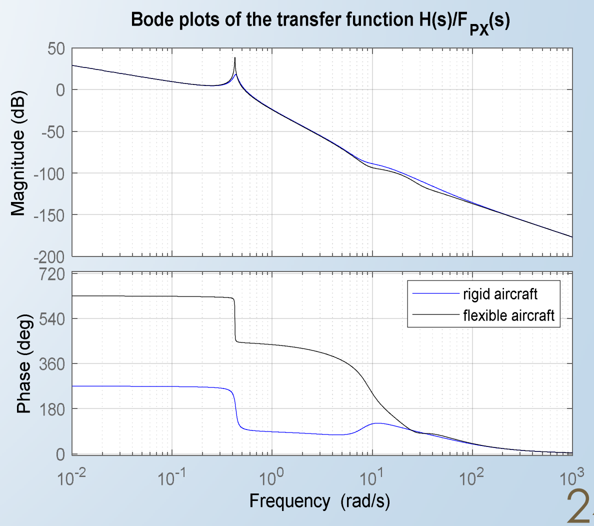

Elevator-to-state-variables **frequency response**

In this case, both the **magnitude and phase plots** not differ significantly by the presence of the flexible mode.

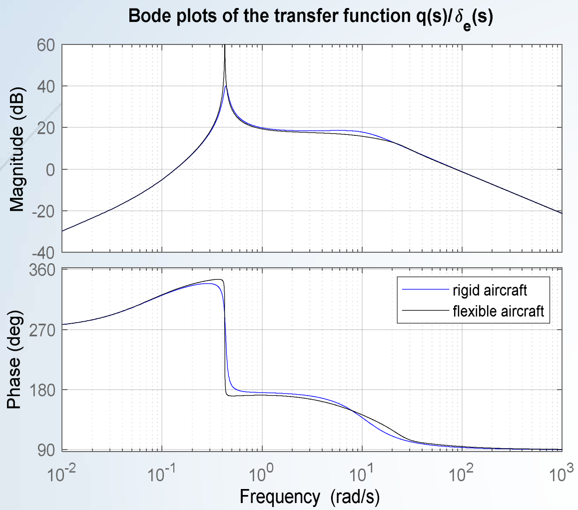

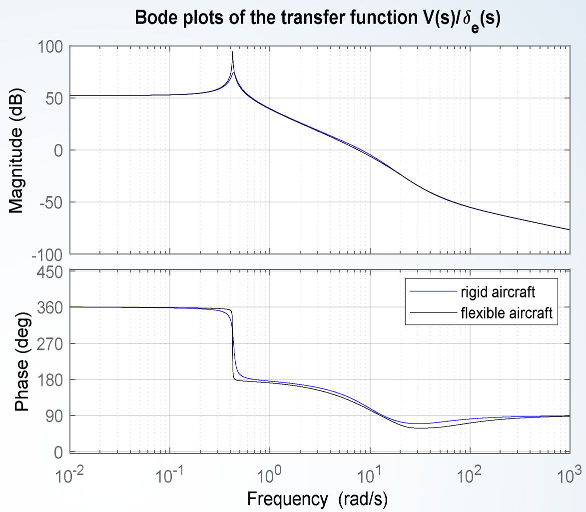

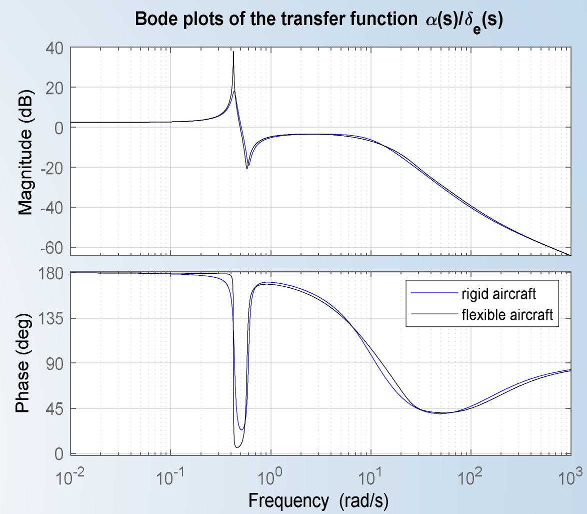

This means that in this operation point the structural flexibility does not appear in time responses and should not be so detrimental to the **control system design** based only in rigid dynamic a priori.

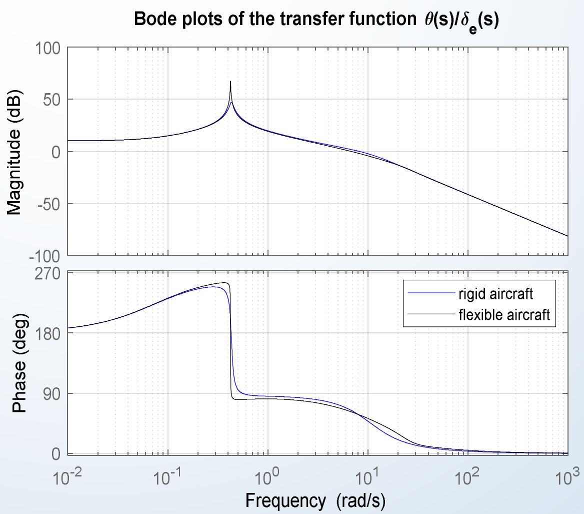

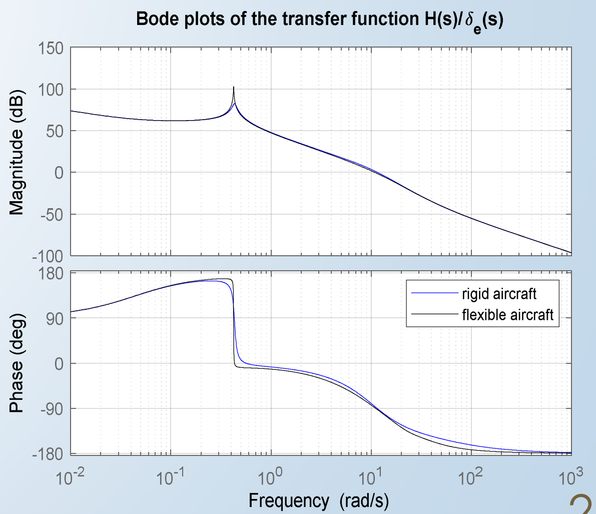

At this point, is important to include the effect of the other flexible modes observed preliminary by GVT tests.

DATA GATHERING FOR CLOSED-LOOP SYSTEM IDENTIFICATION

- Closed-loop system data of an picth-atitude autopilot.
- "trim condition: V=13m/s and H=1100m.

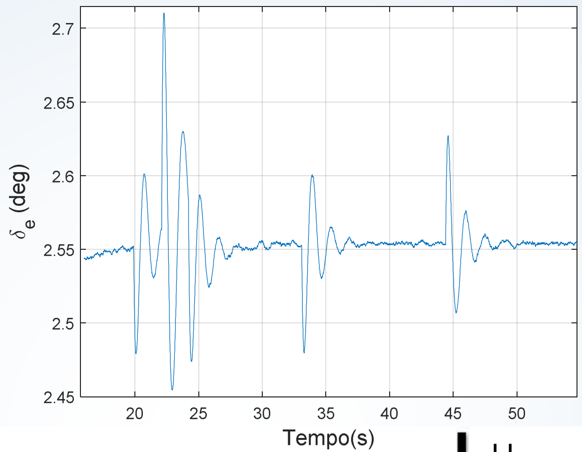

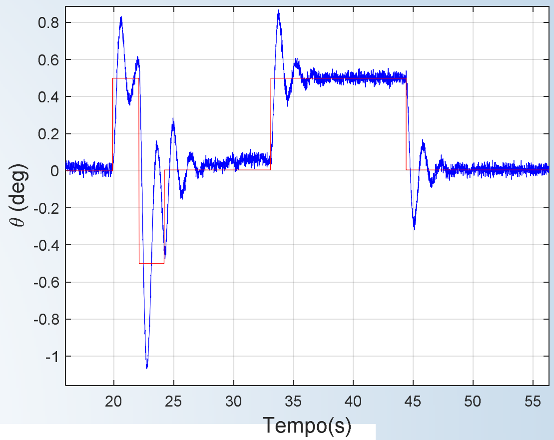

$U_{long} = [\delta_e]$

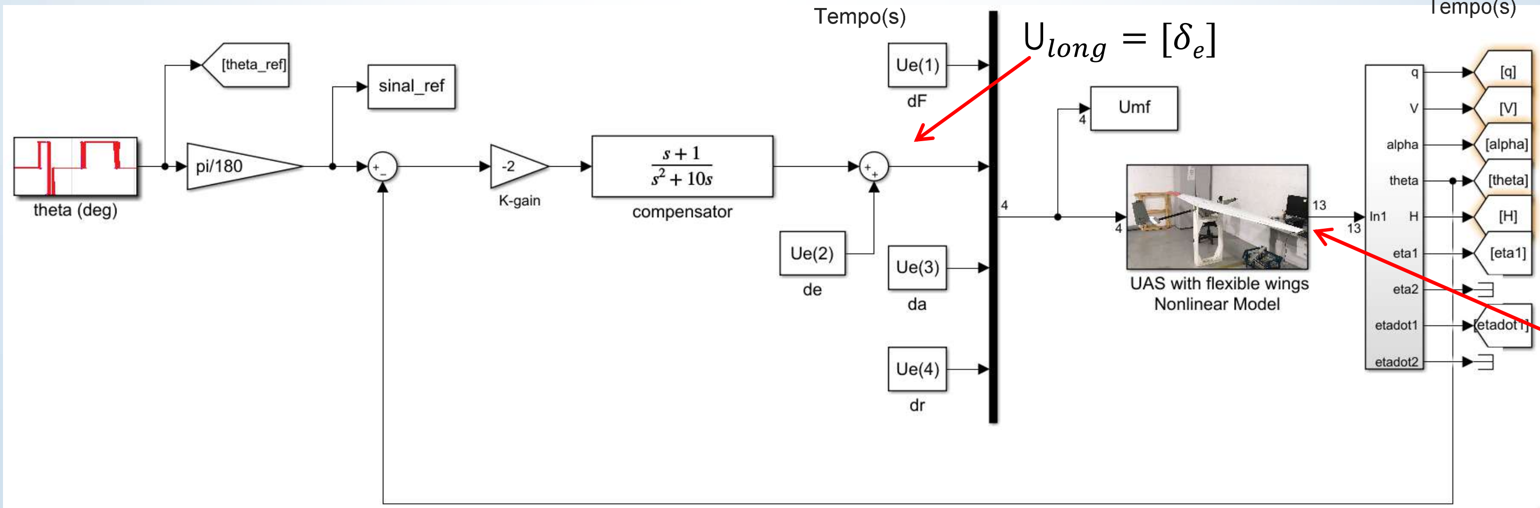

$$Y_{long} = \begin{bmatrix} q \\ V \\ \alpha \\ \theta \\ \eta_i \\ \dot{\eta}_i \end{bmatrix}$$

An attitude-hold autopilot implemented in MATLAB/SIMULINK.

AEROSPACE TECHNOLOGY CONGRESS 2019
SUSTAINABLE AEROSPACE INNOVATION IN A GLOBALISED WORLD
FT2019

IDENTIFICATION – closed loop identification (subspace method)

A subspace method applied both open-loop and closed-loop data named DSR (combined deterministic and stochastic system identification and realization) algorithm.

The system is represented by a discrete-time stochastic linear model as given

$$
\begin{aligned}
x_{k+1} &= \mathrm{A}x_k + \mathrm{B}u_k + \mathrm{K}\varepsilon_k \\
y_k &= \mathrm{C}x_k + \mathrm{D}u_k + \varepsilon_k
\end{aligned}
$$

In formulation of the subspace identification problem, it is necessary to dene an extended state-space model just to generate the data space formed by block Hankel matrices of the input and output data.

$$
\begin{aligned}
\mathrm{X}_{J/1} &= \begin{bmatrix} \tilde{\mathrm{C}}_J^d & \tilde{\mathrm{C}}_J^s \end{bmatrix} \begin{bmatrix} \mathrm{U}_{0/J} \\ \mathrm{Y}_{0/J} \end{bmatrix} + (\mathrm{A} - \mathrm{KD})^J \mathrm{X}_{0/1} \\
\mathrm{Y}_{J/L} &= \tilde{\mathrm{O}}_L \mathrm{X}_{J/1} + \tilde{\mathrm{H}}_L^d \mathrm{U}_{J/L} + \tilde{\mathrm{H}}_L^s \varepsilon_{J/L}
\end{aligned}
$$

IDENTIFICATION – closed loop identification (subspace method)

The projection equation is given by

$$\tilde{O}_L X_{L/1} = R_{32} R_{22}^{\dagger} \begin{bmatrix} U_{0/L} \\ Y_{0/L} \end{bmatrix}$$

Applying a singular value decomposition in the projection matrix

$$R_{32} R_{22}^{\dagger} \begin{bmatrix} U_{0/L} \\ Y_{0/L} \end{bmatrix} = USV^T \approx U_1 S_1 V_1^T$$

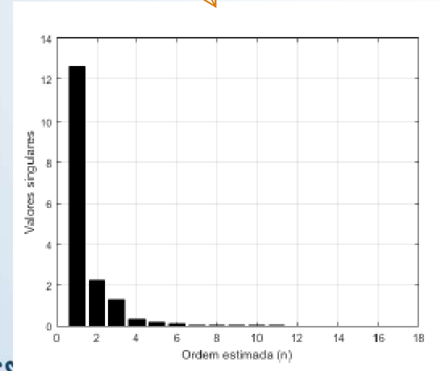

The observability matrix is given by

$$\tilde{O}_L = U_1 S_1^{\frac{1}{2}} \rightarrow C = \tilde{O}_L(1:l, 1:n)$$

An estimated state sequence of the sytem is

$$\tilde{X}_{J/1} = S_1^{\frac{1}{2}} V_1^T$$

Thus, from the input-output data and estimated state sequence, it is possible to solve the least-squares problem to determine the system matrices $\mathbf{A} \in \Re^{n \times n}$, B $\in \Re^{n \times m}$ and the filter Kalman gain $\mathbf{K} \in \Re^{n \times l}$ up to within a similarity transformation.

$$\begin{aligned} x_{k+1} &= Ax_k + \begin{bmatrix} B & K \end{bmatrix} \begin{bmatrix} u_k \\ \varepsilon_k \end{bmatrix} \\ y_k^d &= Cx_k \end{aligned} \longrightarrow [\mathbf{A}\ \mathbf{B}\ \mathbf{K}] = \tilde{\mathbf{X}}_{J+1/1} / \begin{bmatrix} \tilde{\mathbf{X}}_{J/1} \\ \mathbf{U}_{J/1(new)} \end{bmatrix}$$

Closed-loop **subspace identification**

Time histories of manuever used for identification and the corresponding **energy espectrum.**

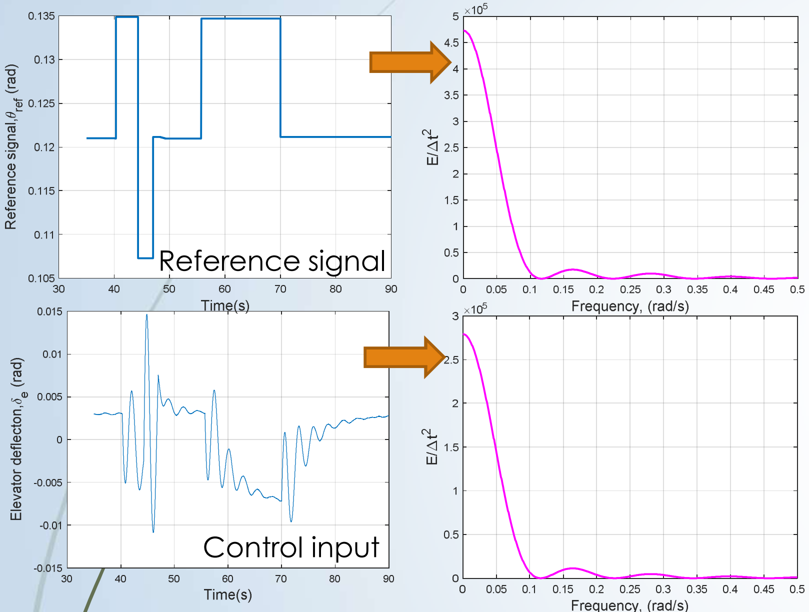

Validation index: the MRSE (mean relative squared error), in percentual (%).

```
ep{y1(k)}=7.54735
ep{y2(k)}=7.13162
ep{y3(k)}=9.31806
ep{y4(k)}=11.1997
ep{y5(k)}=8.54156
ep{y6(k)}=4.86658
ep=8.10081
```

$Y_{long}=[q\ \ V\ \ \alpha\ \theta\ \ \eta_i\ \ \dot{\eta}_i]^T$

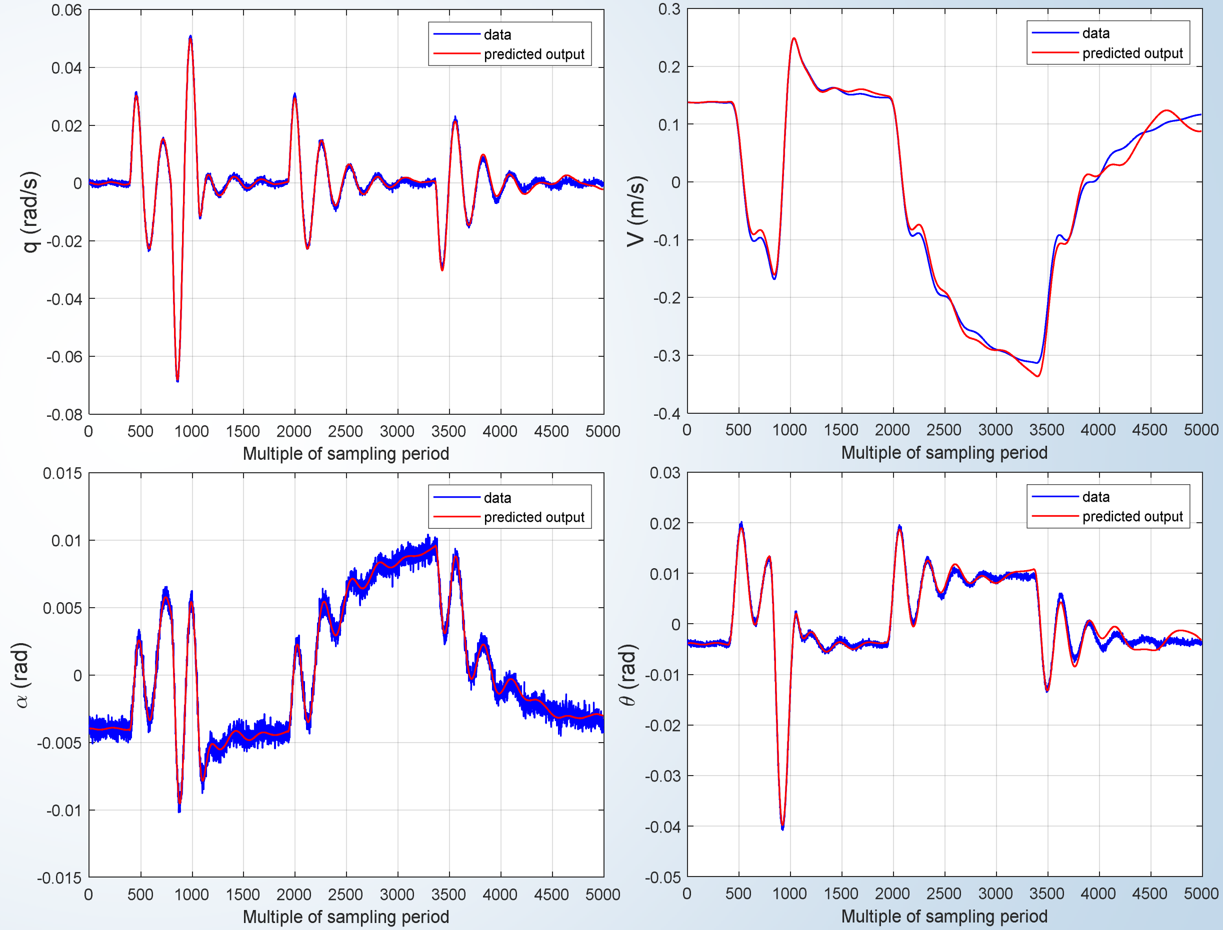

Model output prediction using the **DSR_e algorithm**.

AEROSPACE TECHNOLOGY CONGRESS 2019
SUSTAINABLE AEROSPACE INNOVATION IN A GLOBALISED WORLD
FT2019

Closed-loop **subspace identification**

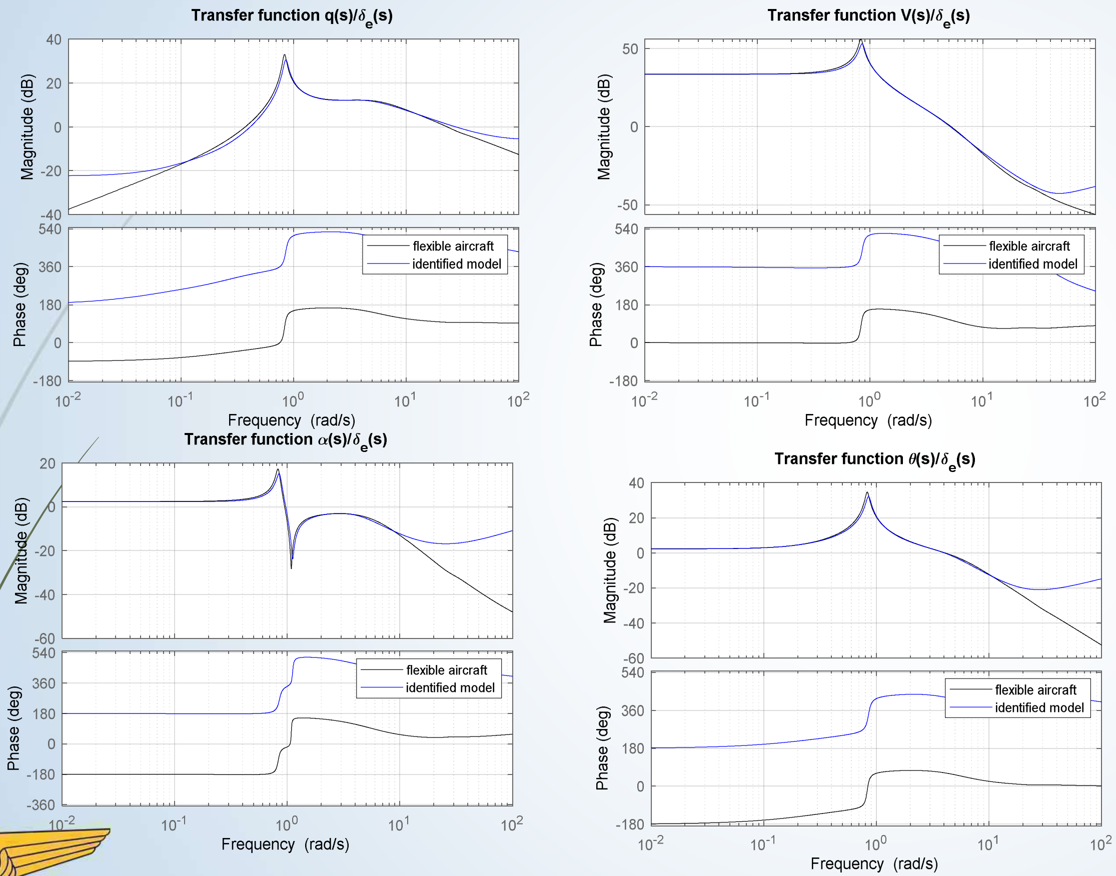

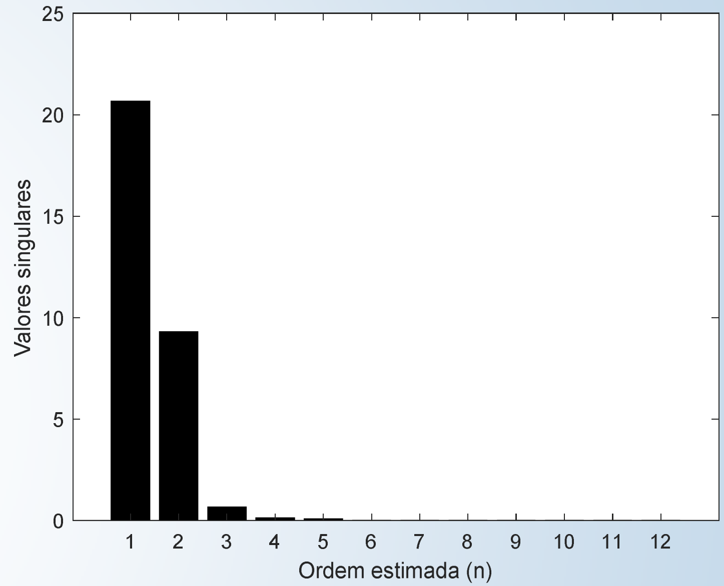

Singular Value Decomposition (SVD) using past horizon J=140 and future horizon L=2. The order n=8 was adopted for the model.

Magnitude and phase plots of the identified model from closed-loop system data corrupted by measurements noise. In blue, the identified model. In black, the simulated preliminary UAS model.

AEROSPACE TECHNOLOGY CONGRESS 2019
SUSTAINABLE AEROSPACE INNOVATION IN A GLOBALISED WORLD
FT2019

L.S.A.
Laboratório de **S**istemas **A**eronáuticos
Aeronautical **S**ystems **L**aboratory

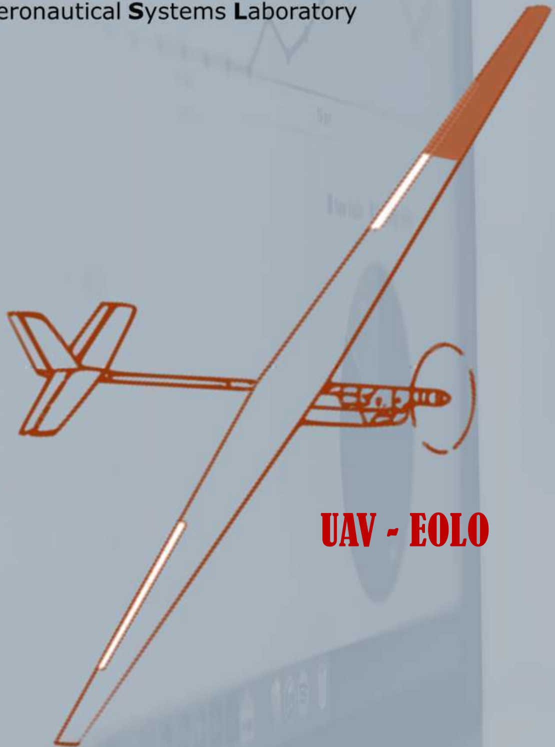

- IDENTIFICATION
- Aerodynamics
- Subspace method
- Modal - GVT EMA
- Modal - GVT OMA

AEROSPACE TECHNOLOGY CONGRESS 2019
SUSTAINABLE AEROSPACE INNOVATION IN A GLOBALISED WORLD
FT2019

IDENTIFICATION – modal (EMA and GVT setup)

Free-free support

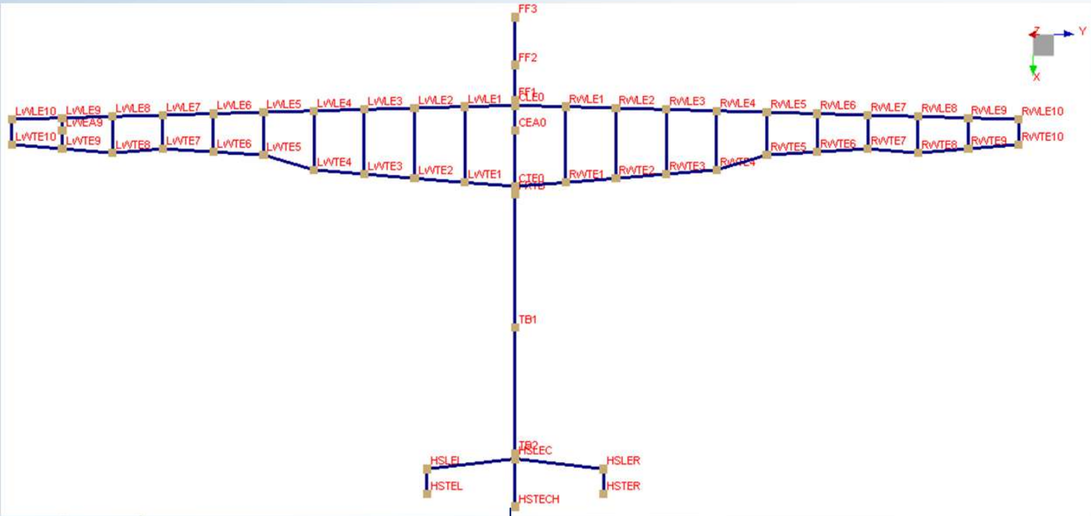

SCADAS LMS

ICP Accelerome ters

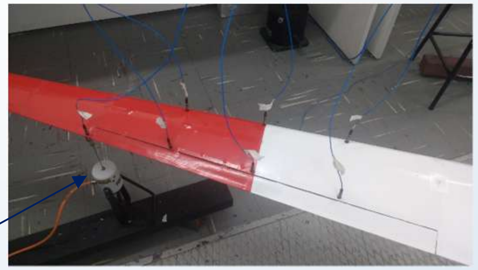

Electromagne tic Shaker and ICP power transducer

IDENTIFICATION – modal (EMA - FRF and Coherence)

Excitation	Estimator	Averages	Windowing	Bandwidth	Spectral lines	Resolution
Burts Random	H1	50	Hanning	50 Hz	1024	0.049 Hz

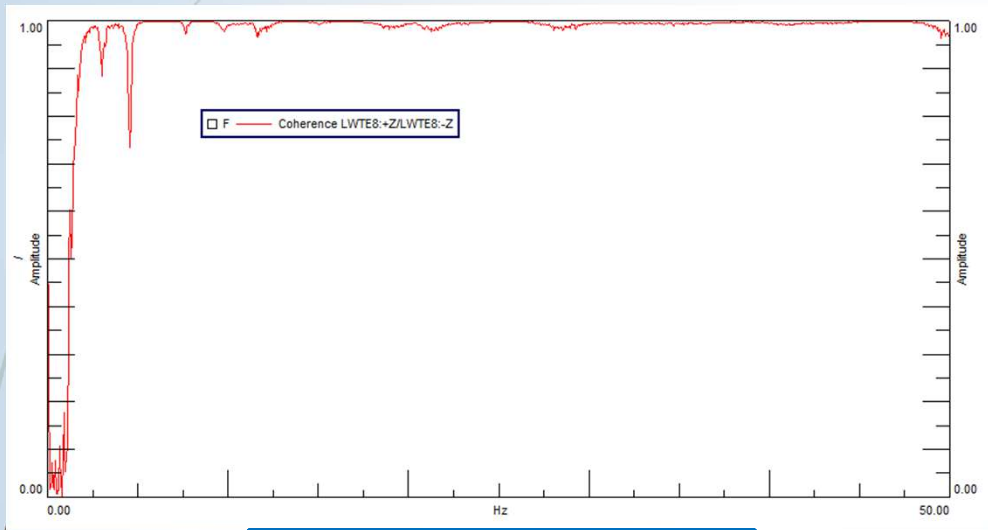

EMA Driving Point Coherence

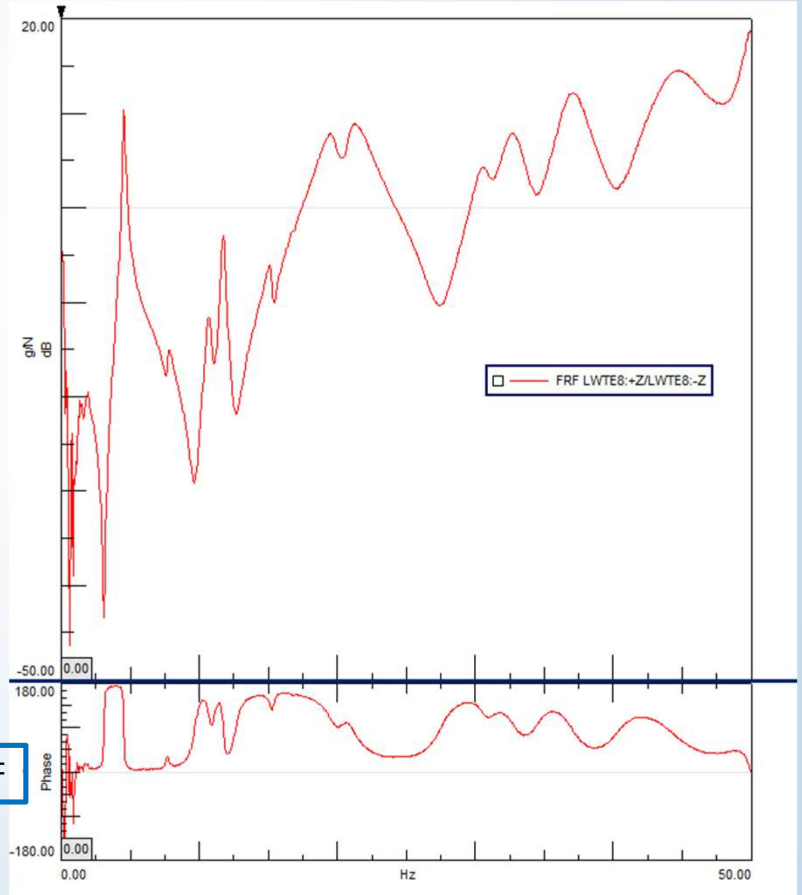

EMA Driving Point FRF

IDENTIFICATION – modal properties from EMA analysis

Mode	Frequency [Hz]	Damping []
1st Symmetrical wing bending	4.6	1.6
Tail-boom torsion	7.7	2.1
1st Anti-symmetrical wing bending + tail-boom torsion	10.6	2.2
1st Anti-symmetrical wing bending + tail-boom torsion	11.6	1.2
1st Symmetrical wing torsion + tail-boom bending	15.0	1.7
1st Anti-symmetrical wing torsion	19.1	3.2
2nd Symmetrical wing bending + Symmetrical wing torsion	21.2	3.8
2nd Anti-symmetrical wing bending	30.4	2.4

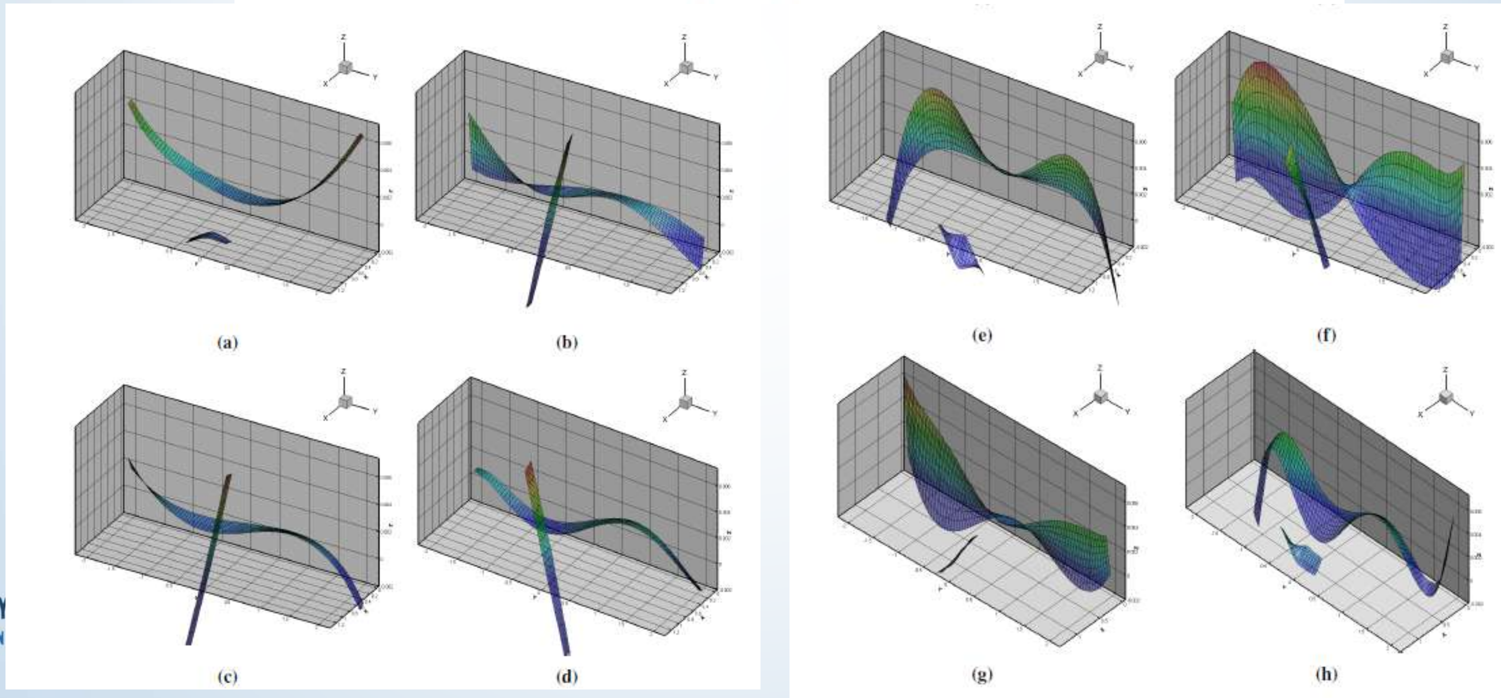

(a) (b) (e) (f)

(c) (d) (g) (h)

L.S.A.
Laboratório de Sistemas Aeronáuticos
Aeronautical Systems Laboratory

- IDENTIFICATION
- Aerodynamics
- Subspace method
- Modal - GVT EMA
- Modal - GVT OMA

IDENTIFICATION – modal (OMA – GVT)

- The supporting system for GVT-OMA was the same that for GVT-EMA
- Excitation with impulsive inputs
- Internal instrumentation was used for response recording.

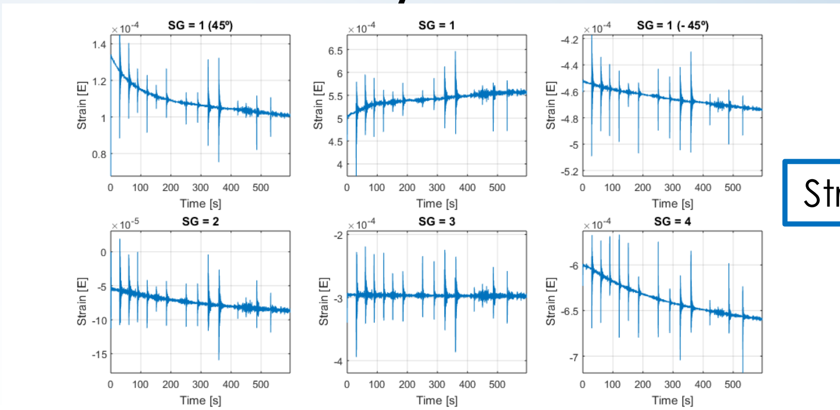

Strain responses

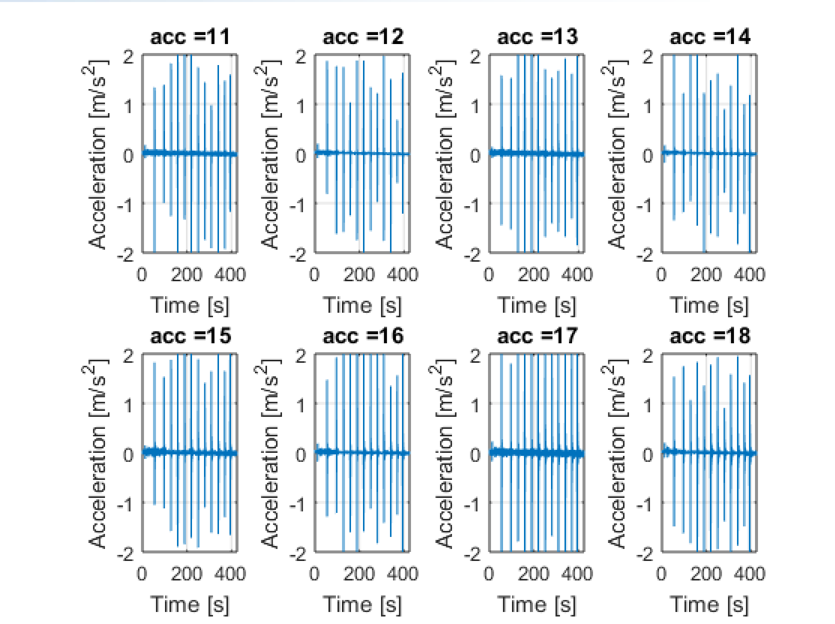

Right semi-wing acceleration responses

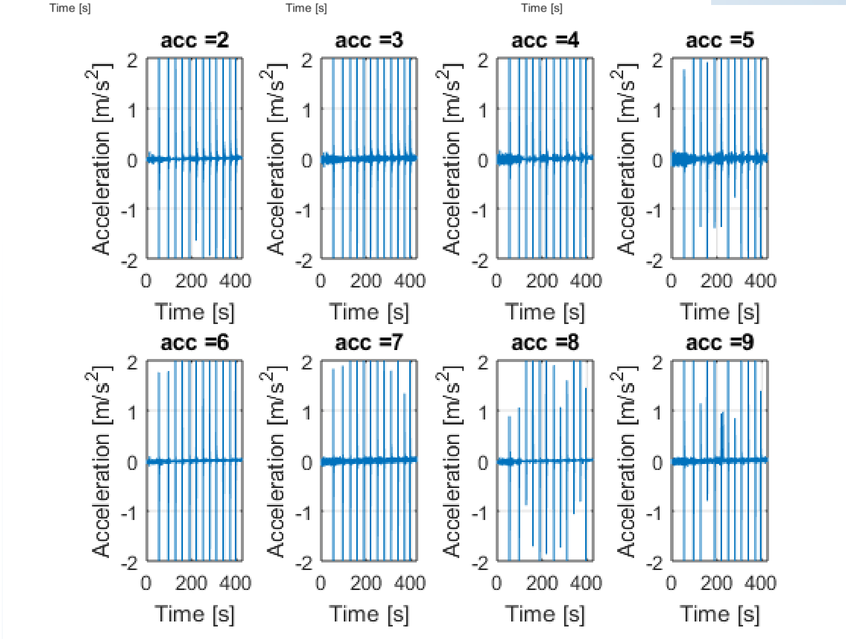

Left semi-wing acceleration responses

IDENTIFICATION – modal properties from OMA Analysis

Mode	Frequency [Hz]	Damping [%]
1st Symmetrical wing bending	4.6	0.7
1st Anti-symmetrical wing bending	11.7	1.9
1st Symmetrical wing torsion	15.1	2.9
1st Anti-symmetrical wing torsion	18.8	3.6
2nd Symmetrical bending + torsion	21.0	3.5

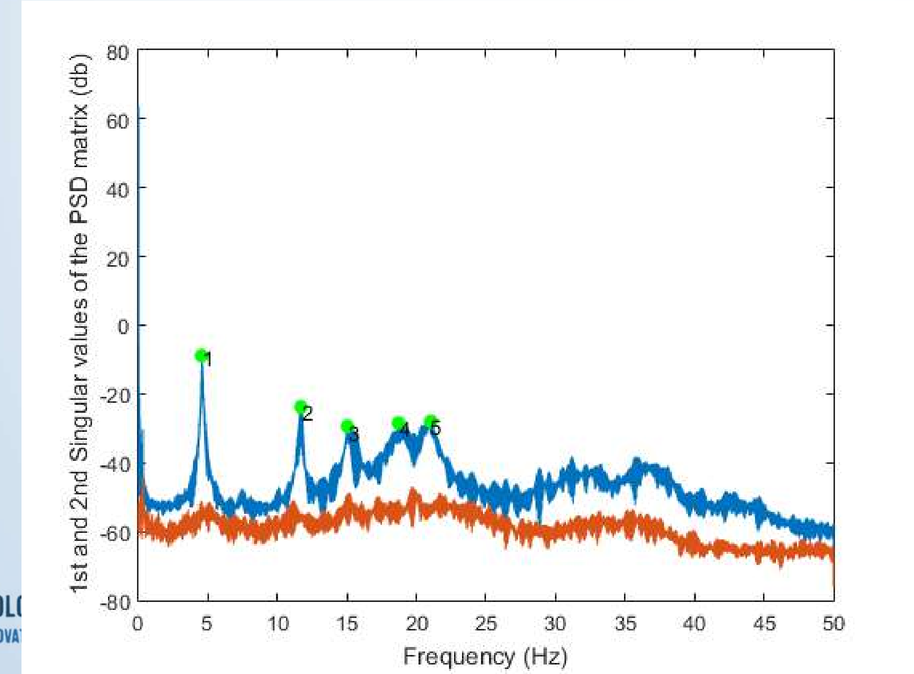

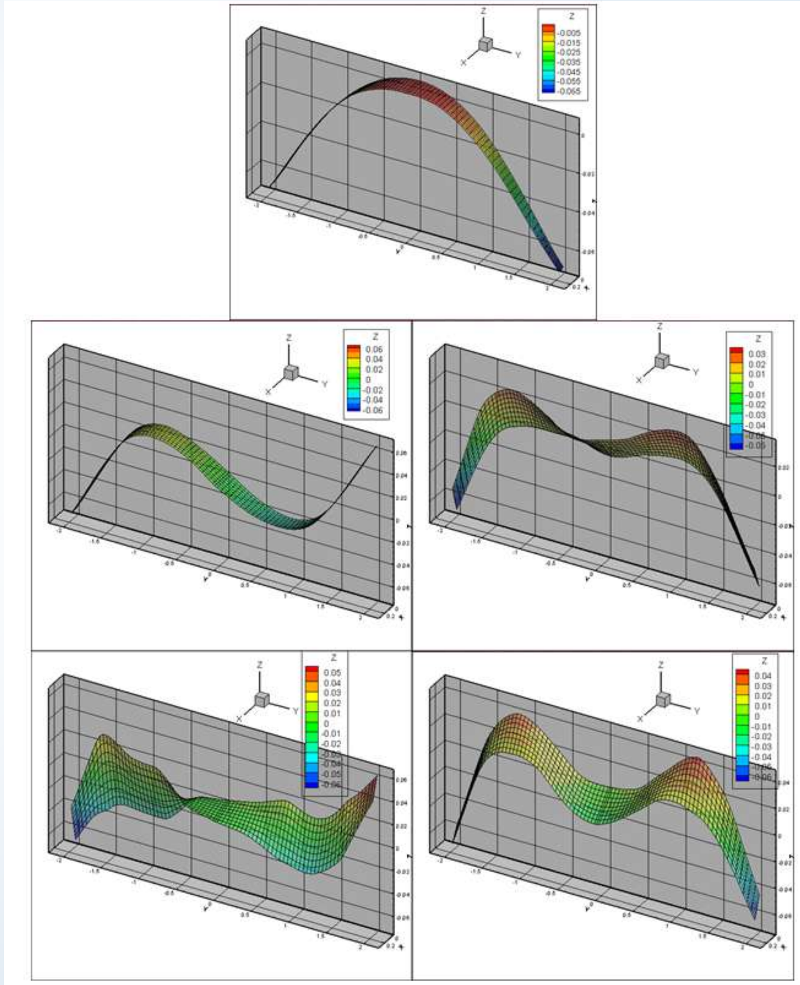

L.S.A.
Laboratório de Sistemas Aeronáuticos
Aeronautical Systems Laboratory

INTRODUCTION

THE EOLO UAV

IDENTIFICATION

WIND TUNEL CAMPAIGN

IN-FLIGHT CAMPAIGN

CONCLUSION

AEROSPACE TECHNOLOGY CONGRESS 2019
SUSTAINABLE AEROSPACE INNOVATION IN A GLOBALISED WORLD
FT2019

WIND TUNEL CAMPAIGN

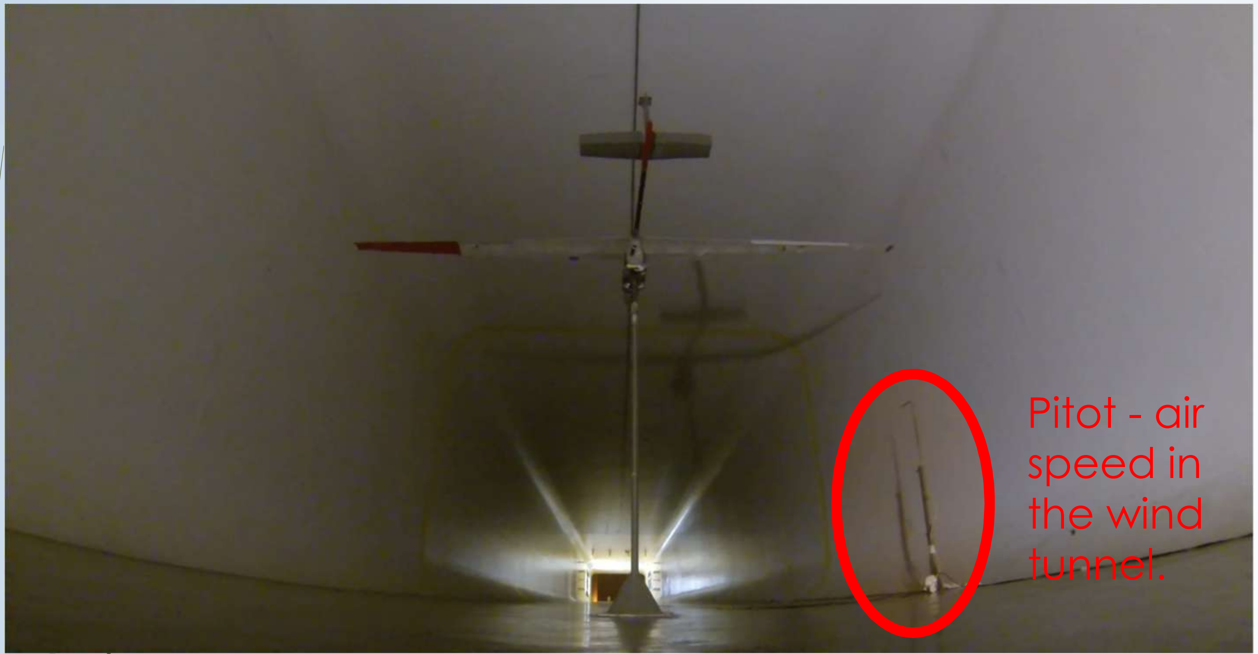

Due to the large wingspan, the test was realized outside the typical section test.

For this essay, it was programmed to increase the speed in 5 km/h for every 2 minutes until a maximum speed at 55 km/h (for the wind tunnel air speed).

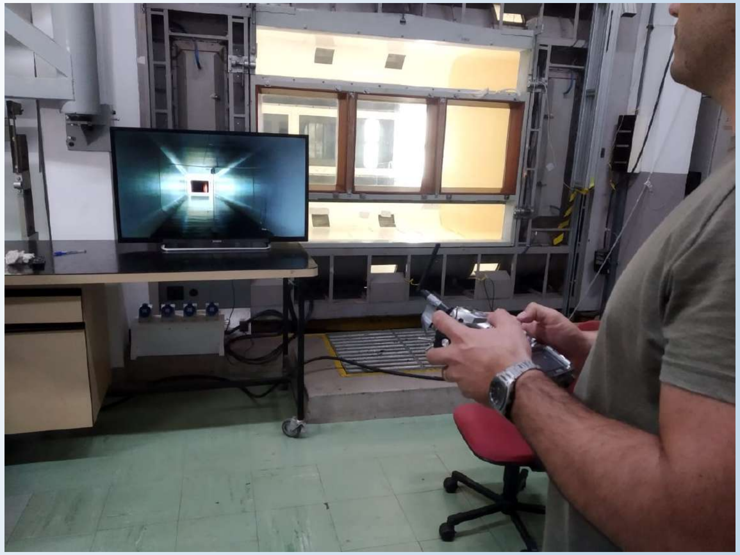

The UAV was being piloted outside the tunnel

WIND TUNEL CAMPAIGN - On board collected data accelerometers

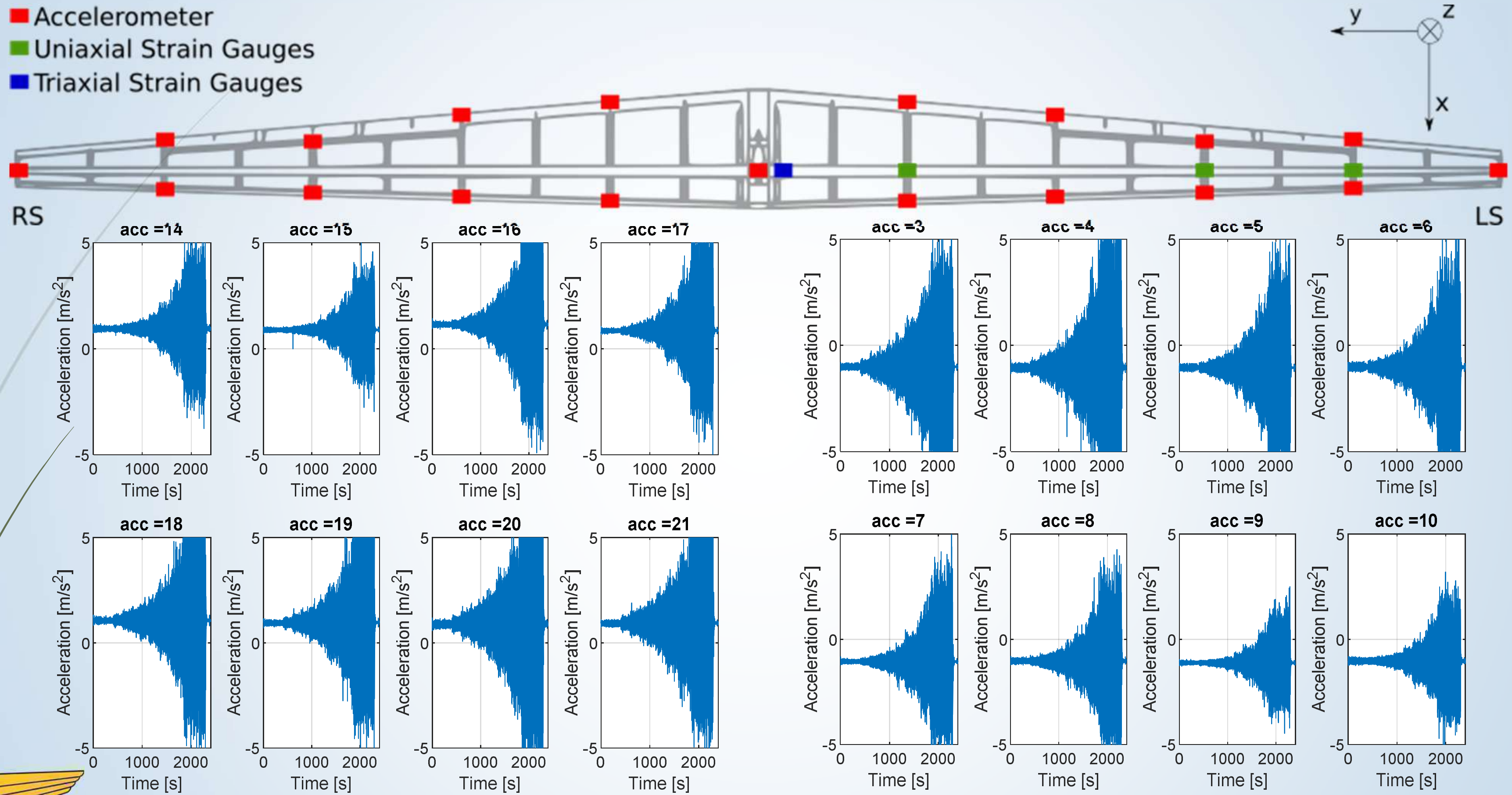

The right side of the wing

The left side of the wing

WIND TUNEL CAMPAIGN - OMA Analysis

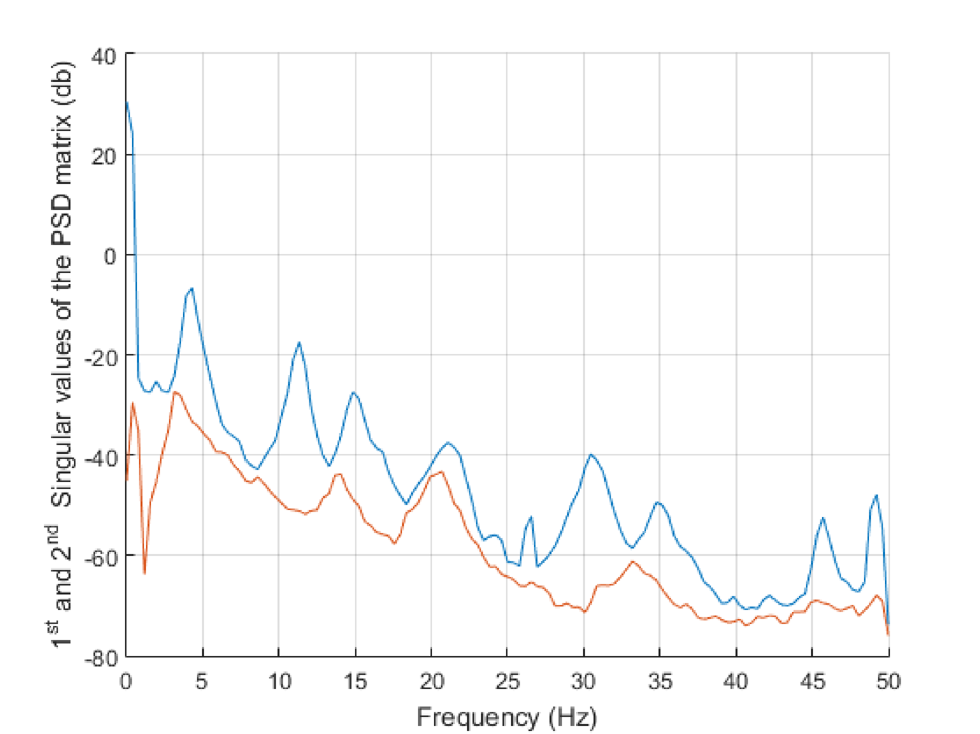

Fdd of the accelerometers data
Wind tunnel air speedy 25 km/h (6.94 m/s)

Mode	Frequency [Hz]
1st wing S bending	4.150
Tail-boom torsion	
1st wing A bending	11.328
1st Fus bending+ 2nd SWB+ SWT	14.966
1st S Torsion	19.605
1st A Torsion + 2nd SWB	21.045
2nd AWB	30.518
3rd SWB	34.888

WIND TUNEL CAMPAIGN - OMA Analysis

Mode	Frequency [Hz]
1st wing S bending	4.688
Tail-boom torsion	
1st wing A bending	11.279
1st Fus bending+ 2nd SWB+ SWT	15.479
1st S Torsion	
1st A Torsion + 2nd SWB	19.678
2nd AWB	30.542
3rd SWB	34.790

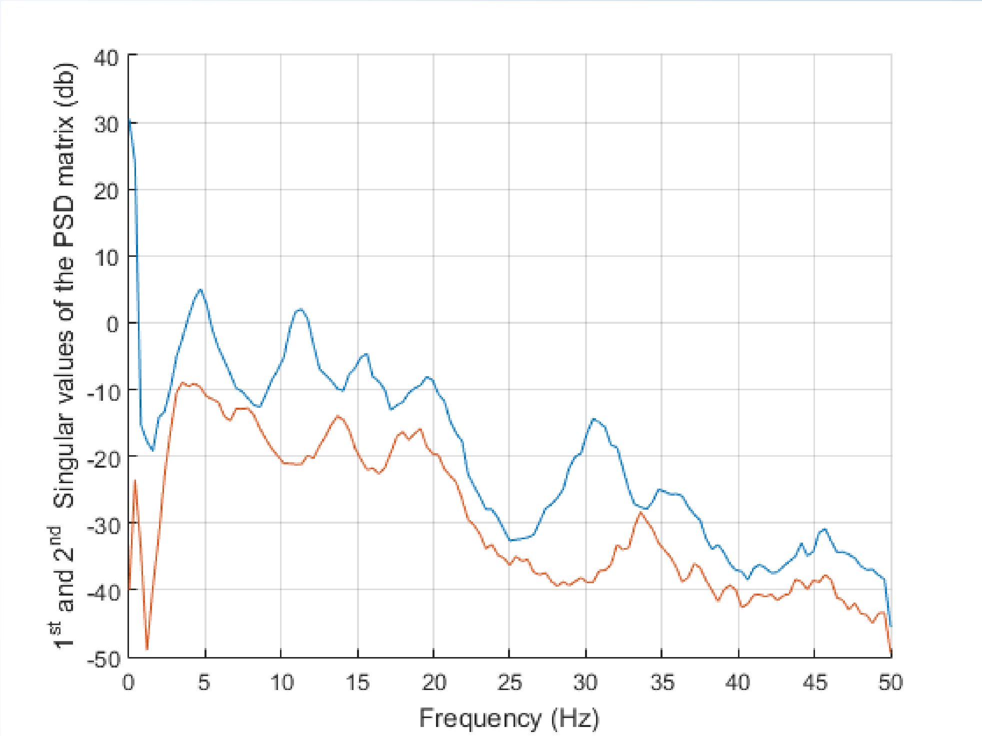

Fdd of the accelerometers data. Wind tunnel air speedy 40 km/h (11,11 m/s)

WIND TUNEL CAMPAIGN - OMA Analysis

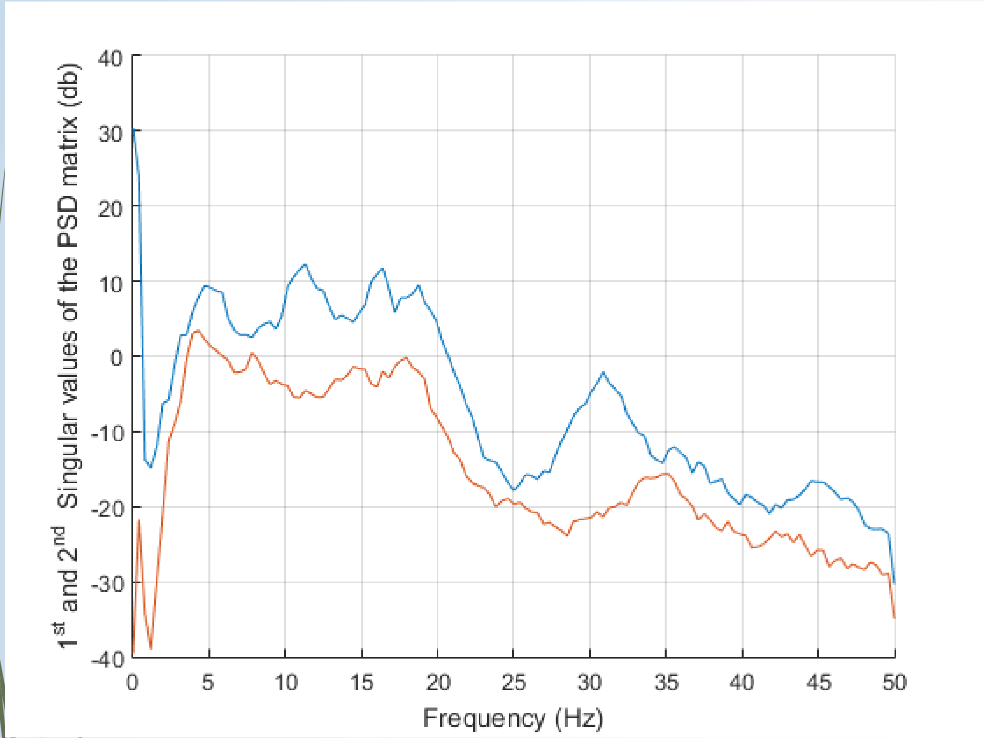

Fdd of the accelerometers data. Wind tunnel air speedy 50 km/h (13.89 m/s)

Mode	Frequency [Hz]
1st wing S bending	4.858
Tail-boom torsion	
1st wing A bending	11.279
1st Fus bending+ 2nd SWB+ SWT	16.382
1st S Torsion	
1st A Torsion + 2nd SWB	18.677
2nd AWB	30.933
3rd SWB	35.425

WIND TUNEL CAMPAIGN - OMA Analysis

Mode	Frequency [Hz]
1st wing S bending	
Tail-boom torsion	
1st wing A bending	
1st Fus bending+ 2nd SWB+ SWT	15.454
1st S Torsion	
1st A Torsion + 2nd SWB	18.555
2nd AWB	31.397
3rd SWB	35.840

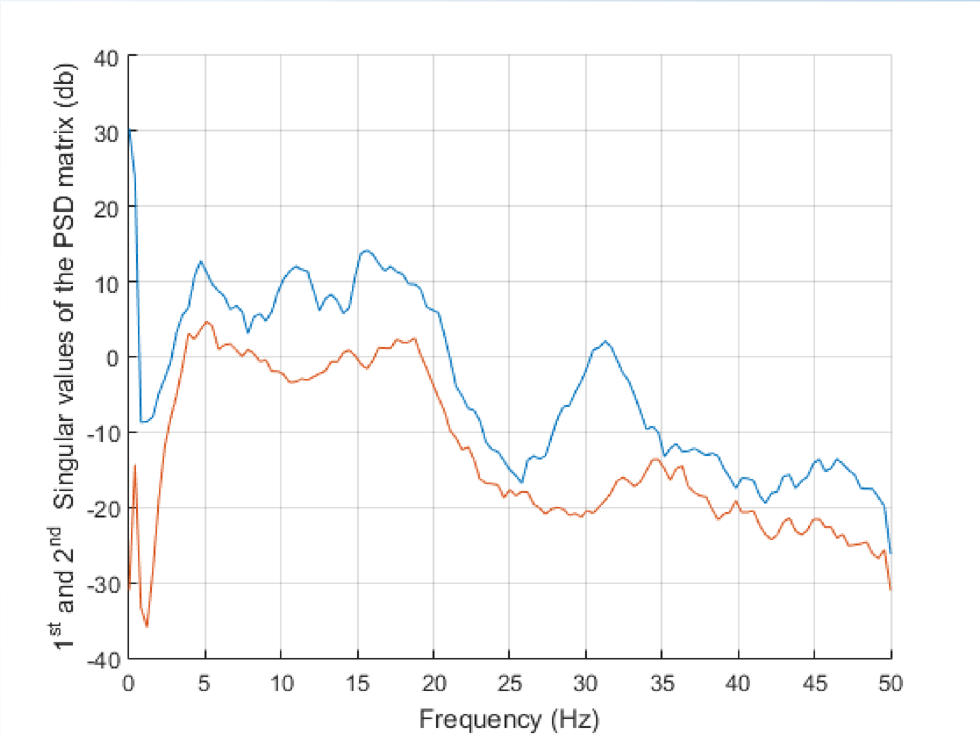

Fdd of the accelerometers data. Wind tunnel air speedy 55 km/h (15,28 m/s)

WIND TUNEL CAMPAIGN - OMA Analysis

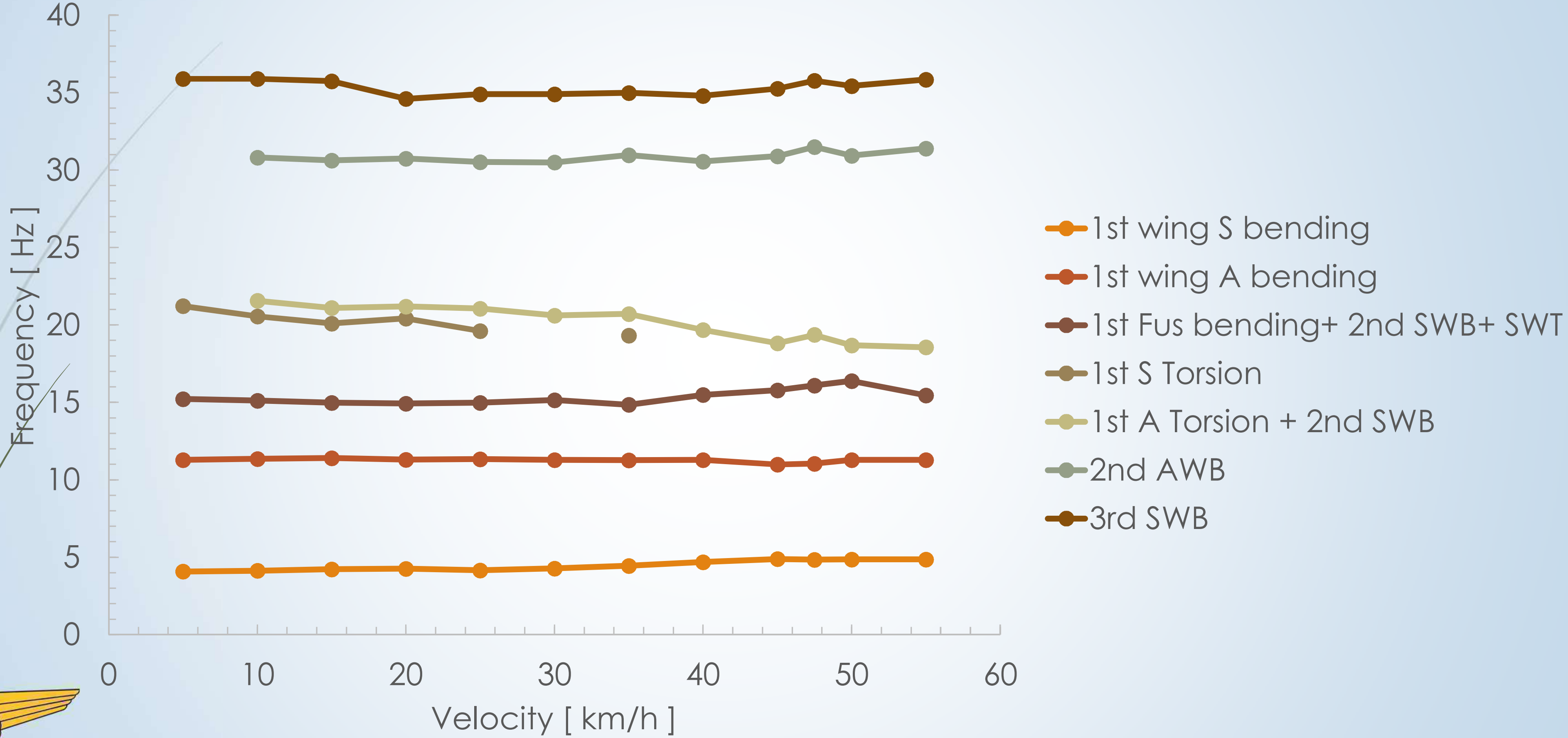

L.S.A.
Laboratório de Sistemas Aeronáuticos
Aeronautical Systems Laboratory

AEROSPACE TECHNOLOGY CONGRESS 2019
SUSTAINABLE AEROSPACE INNOVATION IN A GLOBALISED WORLD
FT2019

IN - FLIGHT CAMPAIGN

IN - FLIGHT CAMPAIGN - OMA Analysis

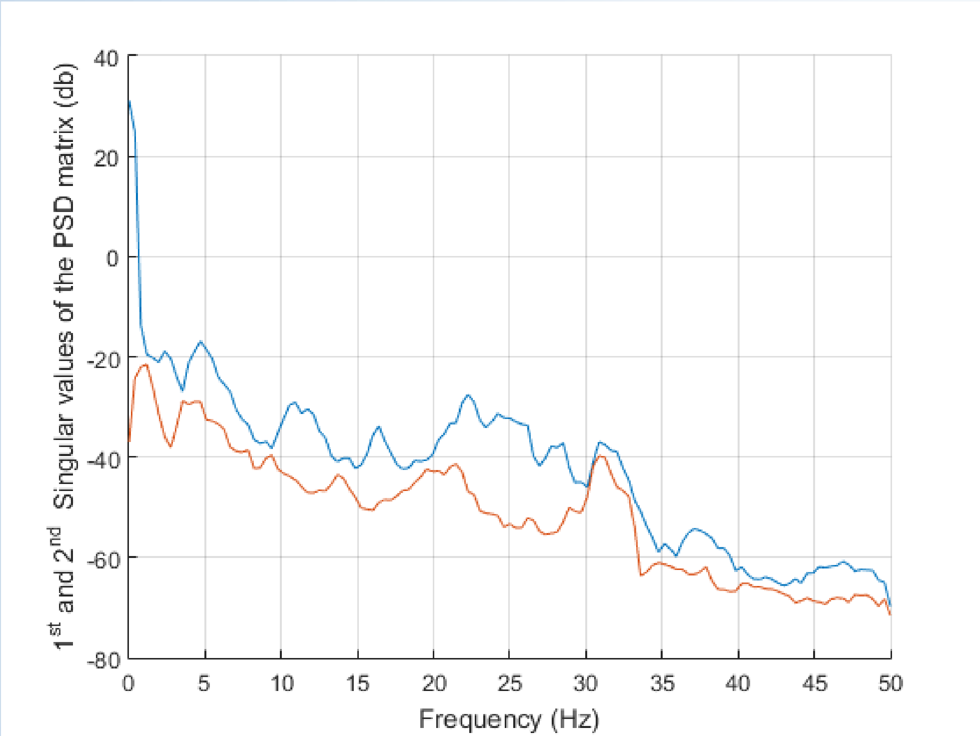

Fdd of the accelerometers data Air speedy 25 knots (12.86 m/s)

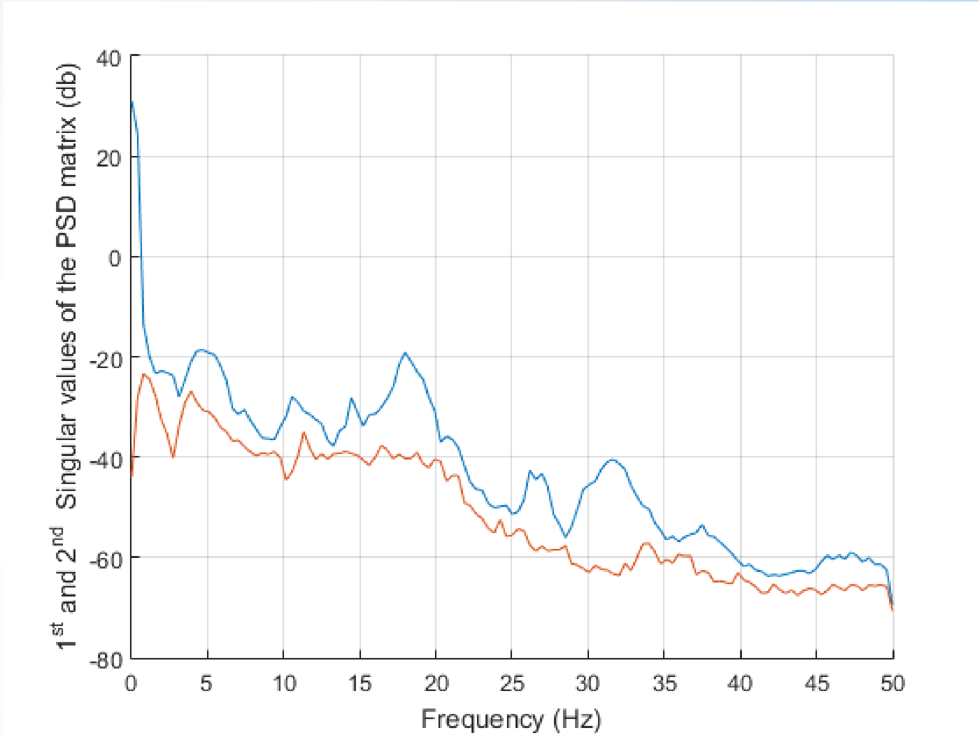

Fdd of the accelerometers data Air speedy 30 knots (15.43 m/s)

IN - FLIGHT CAMPAIGN - OMA Analysis

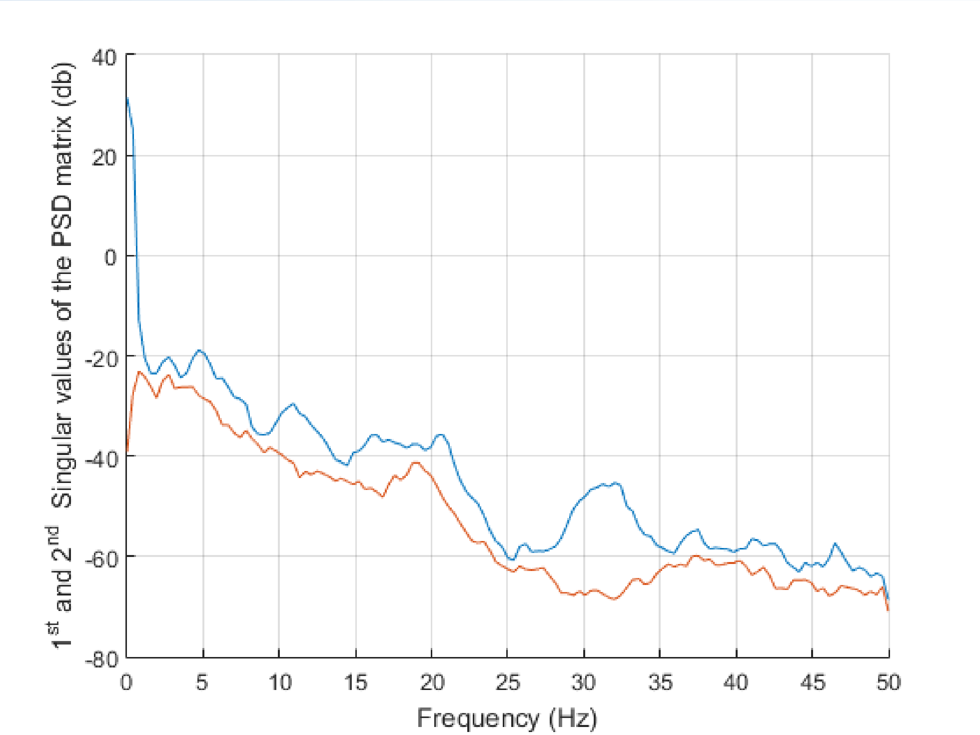

Fdd of the accelerometers data Air speedy 35 knots (18.00 m/s)

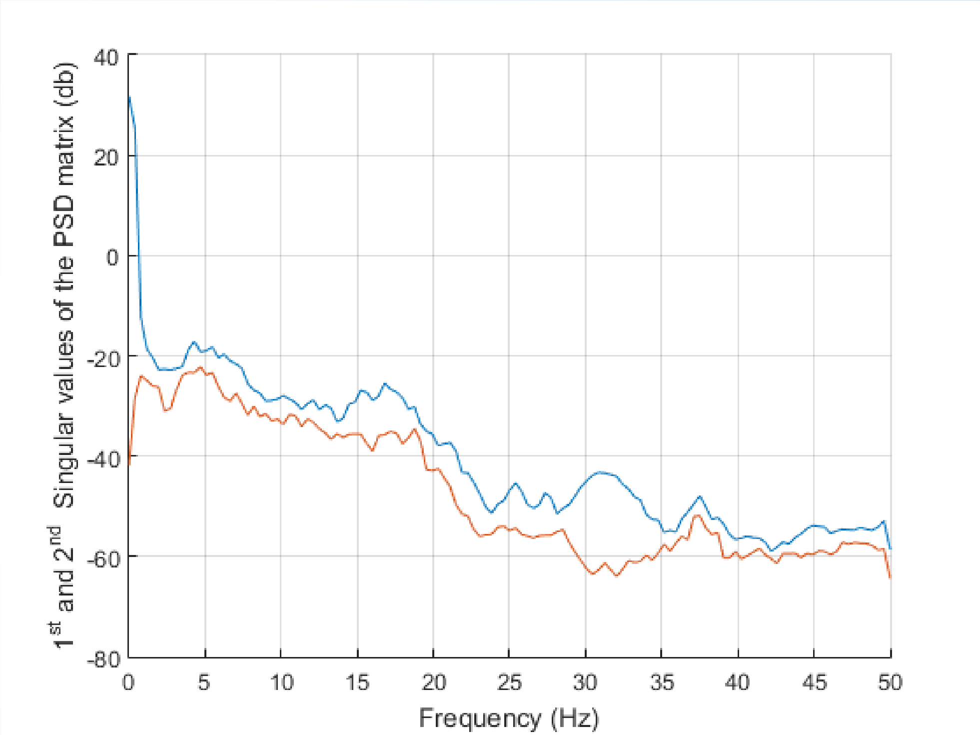

Fdd of the accelerometers data Air speedy 40 knots (20.57 m/s)

L.S.A.
Laboratório de Sistemas Aeronáuticos
Aeronautical Systems Laboratory

INTRODUCTION

THE EOLO UAV

IDENTIFICATION

WIND TUNEL CAMPAIGN

IN-FLIGHT CAMPAIGN

CONCLUSION

CONCLUSION AND ONGOING WORKS

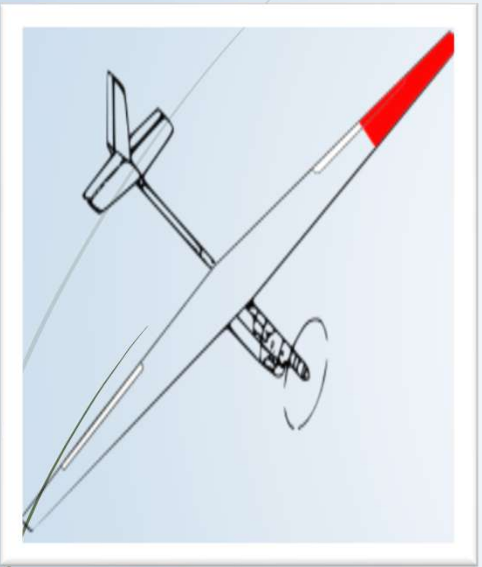

This article is ongoing research that will consist of validating the simulator dynamic using experimental data.

From the synthetics data, it was possible to apply the EKF method to identification of the aerodynamics derivatives and compare them with well known the results such as AVL and Waszack formulation.

The model identification with the subspace model swas applied to synthetic data obtained wit a simulation model using the aerodynamic derivatives calculated by the Waszack formulation and also with AVL simulation. Both models considered just one flexible mode. With the GVT and the wind tunnel campaign it was possible to identify seven flexibles modes. The in-flight test has just started, and a first analysis shows approximately the same modal behavior,

The next step of this research will be the complete identification of aerodynamics and control derivatives using in-flight data and a theorical considering more flexible modes.

L.S.A.
Laboratório de Sistemas Aeronáuticos
Aeronautical Systems Laboratory

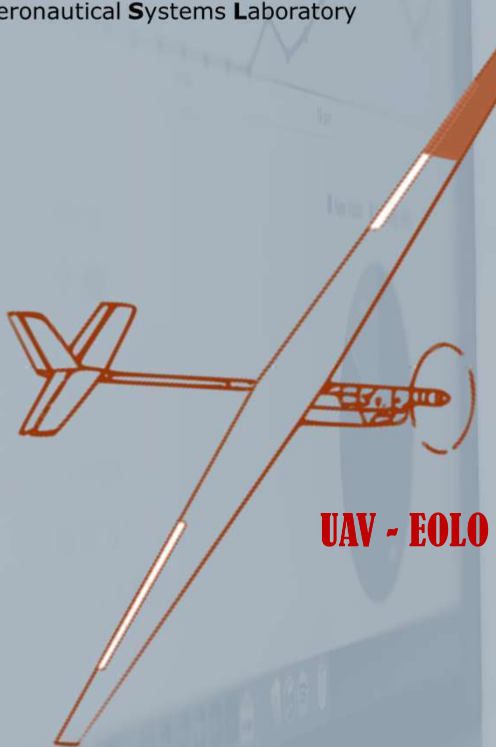

AEROSPACE TECHNOLOGY CONGRESS 2019
SUSTAINABLE AEROSPACE INNOVATION IN A GLOBALISED WORLD
FT2019

REFERENCES

AEROSPACE TECHNOLOGY CONGRESS 2019
SUSTAINABLE AEROSPACE INNOVATION IN A GLOBALISED WORLD
FT2019

BARBOSA, R. C. M. G.; GOES, L. C. S. (2018)
Closed-loop system identification of a large flexible aircraft using subspace methods. ICAS 2018

BARBOSA, R. C. M. G.; GOES, L. C. S. ; SOUSA, M. S. (2019)
Closed-loop System Identification of an Unmanned Aerial System (UAS) with Flexible Wings using Subspace Methods. DINAME 2019

Souza, A. G.; D. C. Zuniga ; GOES, L. C. S. ; SOUSA, M. S. (2019)
Parameter Identification for a Flexible Unmanned Aerial Vehicle Using Extended Kalman Filtering DINAME 2019

D. C. Zuniga. ; Souza, A. G; GOES, L. C. S. (2019)
Development of an Aeroelastic In-Flight Testing System for a Flexible Wing Unmanned Aerial Vehicle using Acceleration and Strain Sensors AIAA 2019

D. C. Zuniga. ; Souza, A. G; GOES, L. C. S. (2019)
Operational Modal Analysis using Impulsive Input of a Flexible Wing Unmanned Aerial Vehicle DINAME 2019

D. C. Zuniga. ; Souza, A. G; GOES, L. C. S. (2019)
Flight dynamics modeling of a flexible wing unmanned aerial vehicle ICEDYN 2019

D. C. Zuniga. ; Souza, A. G; GOES, L. C. S. (2019)
Planning of an in-flight aeroelastic testing of a flexible unmanned aerial vehicle using a combined accelerometers-strain sensors operational modal analysis ICEDYN 2019

Souza, A. G.; D. C. Zuniga ; GOES, L. C. S. ; SOUSA, M. S. (2018)
Identificação de parâmetro da dinâmica longitudinal de uma aeronave flexível usando o método de erro na saída CONEM 2018

CAPES
VINNOVA
Finep
FINANCIADORA DE INOVAÇÃO E PESQUISA
MINISTÉRIO DA CIÊNCIA, TECNOLOGIA, INOVAÇÕES E COMUNICAÇÕES
PÁTRIA AMADA BRASIL
GOVERNO FEDERAL

Thank you for your attention...

L.S.A.
Laboratório de **S**istemas **A**eronáuticos
Aeronautical **S**ystems **L**aboratory

AEROSPACE TECHNOLOGY CONGRESS 2019
SUSTAINABLE AEROSPACE INNOVATION IN A GLOBALISED WORLD
FT2019

Questions?

Prof. Luiz Carlos Sandoval Góes
goes@ita.br
Aeronautics Institute of Technology – ITA
Department of Mechanical Engineering (IEM)